

1 **Title:** Continental-scale plant invasions reshuffle the soil microbiome of blue carbon
2 ecosystems

3

4 **Running Title:** Soil microbiome after plant invasions

5

6 **Authors:** Gui-Feng Gao^{1, 2, 3, #}, Huan Li^{3, 4, #}, Yu Shi⁵, Teng Yang^{1, 2}, Chang-Hao Gao³,
7 Kunkun Fan^{1, 2}, Yihui Zhang³, Yong-Guan Zhu⁶, Manuel Delgado-Baquerizo^{7, 8, *},
8 Hai-Lei Zheng^{3, *}, Haiyan Chu^{1, 2, *}

9 [#]These authors contributed equally to this work.

10

11 ¹ State Key Laboratory of Soil and Sustainable Agriculture, Institute of Soil Science,
12 Chinese Academy of Sciences, 71 East Beijing Road, Nanjing 210008, China

13 ² University of Chinese Academy of Sciences, Beijing 100049, China

14 ³ Key Laboratory of the Ministry of Education for Coastal and Wetland Ecosystems,
15 College of the Environment and Ecology, Xiamen University, Xiamen 361102, China

16 ⁴ College of Food and Bio-engineering, Bengbu University, Bengbu 233030, China

17 ⁵ State Key Laboratory of Crop Stress Adaptation and Improvement, School of Life
18 Sciences, Henan University, Kaifeng 475004, China

19 ⁶ Key Laboratory of Urban Environment and Health, Institute of Urban Environment,
20 Chinese Academy of Sciences, Xiamen 361021, China

21 ⁷ Laboratorio de Biodiversidad y Funcionamiento Ecosistemico. Instituto de Recursos
22 Naturales y Agrobiología de Sevilla (IRNAS), CSIC, Av. Reina Mercedes 10, E-
23 41012, Sevilla, Spain

24 ⁸ Unidad Asociada CSIC-UPO (BioFun). Universidad Pablo de Olavide, 41013
25 Sevilla, Spain

26

27 Email list:

28 Gui-Feng Gao, gfgao@issas.ac.cn

29 Huan Li, huanlee723@stu.xmu.edu.cn
30 Yu Shi, yshi@henu.edu.cn
31 Teng Yang, tyang@issas.ac.cn
32 Chang-Hao Gao, 33120170155158@stu.xmu.edu.cn
33 Kunkun Fan, kkfan@issas.ac.cn
34 Yihui Zhang, zyh@xmu.edu.cn
35 Yong-Guan Zhu, ygzhu@iue.ac.cn
36
37 ORCID list:
38 Gui-Feng Gao, <https://orcid.org/0000-0002-8406-8330>
39 Huan Li, <https://orcid.org/0000-0002-8797-0258>
40 Yu Shi, <https://orcid.org/0000-0001-9612-8321>
41 Teng Yang, <https://orcid.org/0000-0002-8617-4698>
42 Chang-Hao Gao, <https://orcid.org/0000-0001-6910-368X>
43 Kunkun Fan, <https://orcid.org/0000-0002-2922-269X>
44 Yihui Zhang, <https://orcid.org/0000-0002-8710-2151>
45 Yong-Guan Zhu, <https://orcid.org/0000-0003-3861-8482>
46 Manuel Delgado-Baquerizo, <https://orcid.org/0000-0002-6499-576X>
47 Hai-Lei Zheng, <https://orcid.org/0000-0001-8588-1529>
48 Haiyan Chu, <https://orcid.org/0000-0001-9004-8750>
49
50 * Corresponding authors:
51 Haiyan Chu, hychu@issas.ac.cn, (025)-86881356
52 Hai-Lei Zheng, zhenghl@xmu.edu.cn, (0592)-2181005
53 Manuel Delgado-Baquerizo, m.delgadobaquerizo@gmail.com

54 **Abstract**

55 Theory and experiments support that plant invasions largely impact aboveground
56 biodiversity and function. Yet, much less is known on the influence of plant invasions
57 on the structure and function of the soil microbiome of coastal wetlands, one of the
58 largest major reservoirs of biodiversity and carbon on Earth. We studied the
59 continental-scale invasion of *Spartina alterniflora* (SA) across 2,451 km of Chinese
60 coastlines as our model-system, and found that SA invasion can largely influence the
61 soil microbiome (across six depths from 0-100 cm), compared with the most common
62 microhabitat found before invasion (mudflats, Mud). In detail, SA invasion was
63 positively associated with bacterial richness, but also resulted in important biotic
64 homogenization of bacterial communities, suggesting plant invasion can lead to
65 important continental scale trade-offs in the soil microbiome. We found that plant
66 invasion changed the community composition of soil bacterial communities across the
67 soil profile. Moreover, the bacterial communities associated with SA invasions were
68 less responsive to climatic changes than those in native Mud microhabitats,
69 suggesting that these new microbial communities might become more dominant under
70 climate change. Plant invasion also resulted in important reductions in the complexity
71 and stability of microbial networks, decoupling the associations between microbes
72 and carbon pools. Taken together, our results indicated that plant invasions can largely
73 influence the microbiome of coastal wetlands at the scale of China, representing the
74 first continental-scale example on how plant invasions can reshuffle the soil
75 microbiome, with consequences for the myriad of functions that they support.

76

77 **Keywords**

78 Coastal wetland, *S. alterniflora*, Microbial biogeography, Biotic homogenization,
79 Ecological networks, Soil carbon

80

81 **1. Introduction**

82 Coastal wetlands are considered fundamental blue carbon ecosystems playing key
83 roles in regulating carbon sequestration, and supporting biodiversity and ecosystem
84 productivity worldwide (Alongi, 2014; Schuerch et al., 2018). Coastal wetlands are
85 highly vulnerable to many aspects of climate change and human activity, due to their
86 pioneering positions in the intertidal zones (Osland et al., 2016). Among these threats,
87 invasive plant species is one of the most important. Strikingly, although the influences
88 of plant invasions are well described for aboveground biodiversity and functions
89 (Chen et al., 2004; He et al., 2007), much less is known their impacts on the structure
90 and function of the soil microbiome—the largest reservoir of biodiversity on Earth.
91 Here, we used the invasion of *Spartina alterniflora* (SA), native to the southeastern
92 coastline of the United States, through the entire coastline of China as a model system
93 to investigate the impact of plant invasions on the soil microbiome across contrasting
94 climatic conditions.

95 SA was first introduced to China in 1979 for ecological engineering, and has
96 expanded rapidly and extensively along most coastlines of China over the last few
97 decades, encroaching large areas of native bare mudflats (vegetation-free, Mud
98 hereafter) (An et al., 2007; Liu et al., 2018). SA is a perennial herb with a well-
99 developed root system that could reach up to 100 cm underground. The
100 microenvironment varies greatly across different soil depths, such as oxygen status.
101 Thus, the study of the vertical distribution of soil microorganisms before and after SA
102 invasion is important for an in-depth understanding of the ecological consequences of
103 SA invasion. Currently, the distribution area of SA in mainland China has reached
104 545.80 km² by 2015 (Liu et al., 2018), ranging from Liaoning province to Guangdong
105 province across more than 20 latitudes (Liu et al., 2018; Zuo et al., 2012). We
106 compared the influence of SA to the most common microhabitat found before
107 invasion (i.e., Mud; Fig. 1). China has approximately 7,474.6 km² of coastal wetlands,
108 dominated by 5,379.8 km² of Mud microhabitats (Wang et al., 2020). By doing so, we

109 conducted the first continental-scale example on how soil microbiome responds to
110 plant invasions. The extensive occupation of SA in coastal wetlands provides a
111 suitable experimental platform for this study to assess the ecological impact of plant
112 invasion on soil microbial communities within its invasive range.

113 In particular, we carried out a standardized field survey across the coastline of
114 China to investigate the impacts of a model-system plant invasion on the soil
115 microbiome. Among all soil organisms, soil bacteria are the most dominant and
116 diverse organisms of the planet, and support multiple ecosystem functions and
117 services such as nutrient cycling, waste decomposition and carbon sequestration.
118 Because of this, we investigated the influence of plant invasions on the diversity,
119 community composition, ecological networks, and function of soil bacterial
120 microbiomes (our model organism) across China's coastline, compared with Mud
121 microhabitats, which were the most common previously found microhabitat in these
122 ecosystems (Fig. 1).

123 To such an end, we conducted a block design study with 12 sites and paired SA
124 and Mud microhabitats across 20 degrees of latitudes along the Chinese coastline. In
125 these locations, we analyzed 407 composite soil samples from six soil depths (across
126 from 0-100 cm). Standardized soil samplings including multiple soil depths at a
127 continental scale are largely lacking in the literature. Biological homogenization
128 associated with plant invasions has been previously observed for plant
129 (Muthukrishnan & Larkin, 2020; Stotz et al., 2019) and animal communities (Leprieur
130 et al., 2007; Olden & Poff, 2004). Also, recent studies have provided evidences of
131 biological homogenization for fungal at local scale (Zhang et al., 2021) and nematode
132 across the coastlines in China (Zhang et al., 2019) associated with plant invasions.
133 Thus, we hypothesized that the invasion of SA can result in an important biotic
134 homogenization of bacteria by creating very similar environments associated with SA
135 microbiomes across the Chinese coast.

136

137 **2. Material and methods**

138 **2.1 Study sites**

139 Based on the extent area of SA distribution in China, a total of 12 sites were selected
140 across more than 20 latitudes (ranging from 20.60 °N to 40.80 °N), including Huludao
141 (HLD, introduced in 1980s), Tanggu (TG, introduced in 1997), Dongying (DY,
142 introduced in 1990), Lianyungang (LYG, introduced in 1982), Yancheng (YC,
143 introduced in 1983), Chongming (CM, introduced in 1995), Yueqing (YQ, introduced
144 in 1983), Xiapu (XP, introduced in 1980), Yunxiao (YX, introduced in 1999), Zhuhai
145 (ZH, introduced in 1980s), Beihai (BH, introduced in 1986), and Zhanjiang (ZJ,
146 introduced in 1980s) site (Fig. 1a). These sites belong to temperate monsoon climate
147 or tropical-subtropical monsoon climate, with a mean annual temperature ranging
148 from 4.17 °C to 23.98 °C (Fig. 1a).

149 At each site, we sampled soils under paired individuals of Mud and SA
150 microsites (Fig. 1b). Within each site, the selected Mud and SA habitats are located at
151 the comparable elevations and experience a similar tidal dynamic. All selected sample
152 sites were in the mid-tide levels, between the neap high tide and neap low tide levels.
153 In the present study, the soil bacteriome of Mud and SA habitats were compared to
154 reflect the ecological consequences of SA invasion on the most common native
155 habitats before invasion for two reasons: 1) Emerging evidence suggest that the
156 expansion of SA in China was mainly converted from Mud habitats; 2) The native
157 plants of China's coastal wetlands are different from North to South, and it is
158 impossible to find consistent native plants at such a large spatial scale. Due to this
159 reason, Mud habitats were selected as our reference habitat to exclude the possible
160 bias caused by native vegetations.

161

162 **2.2 Collection of soil samples and environmental variables**

163 Soil samples were collected in October 2018 following a consistent sampling and

164 processing scheme. Specifically, a quadrat with 50 × 50 meters was established at
165 each site for Mud and SA habitats, respectively (Fig. 1b). Within this quadrat, three
166 replicates for Mud habitat and four replicates for SA habitat were randomly sampled,
167 with at least 15 meters away in geographical distance from each other. Then, around
168 each replicate, five intact soil cores (~within 1 m to the centroid point) were randomly
169 collected by using PVC pipes (5 cm diameter, 100 cm length). Here, considering the
170 highly developed root system of SA that might alters the microbial distributions
171 between soil depths, soil in different depths were collected up to 100 cm maximum. It
172 is important to note that due to the differences in soil textures, individual plots could
173 only be collected to a maximum depth of 40-60 cm. After achieving the soil cores, they
174 were then divided into 6 sections (0-10 cm, 10-20 cm, 20-40 cm, 40-60 cm, 60-80 cm,
175 and 80-100 cm) using a stainless steel knife, referring to different soil depths (Fig. 1c).
176 The corresponding soils from all the 5 soil cores were completely homogenized as a
177 replicate. Soil samples were sealed immediately after removing gravel stones and
178 other debris. Finally, a total of 407 soil samples were obtained, of which 177 and 230
179 samples for Mud and SA habitat, respectively (Table S1). All the soil samples were
180 stored on ice during the transportation.

181 A suite of 18 environmental variables were obtained, including 11 soil properties
182 and 7 climatic factors (Gao et al., 2022). For soil variables, soil temperature of
183 corresponding sample was determined *in-situ* using a mercury thermometer. Soil
184 redox potential (Eh, mV) and salinity/pH were measured by inserting portable probes
185 into the corresponding depth, by using the ExStik™ RE300 (USA) and ExStik™
186 EC500 (USA), respectively. In the laboratory, soil water content was determined by
187 30 °C oven-drying of 50 g fresh soil to a constant weight. The air-dried soils were
188 ground into powder and sieved through a 2 mm mesh sieve. Soil electrical
189 conductivity (EC) was determined at 25 °C by using a conductivity meter (Leici
190 DDS-307, China). Soil organic matter (SOM) was measured based on the loss on
191 ignition at 550 °C for 6 h after 105 °C oven-dried (Heiri et al., 2001). Soil total carbon

192 (TC), total nitrogen (TN) and total sulfur (TS) were determined using a Vario EL III
193 Elemental Analyzer (Elementar, Hanau, Germany), and then the carbon-to-nitrogen
194 ratio (C/N) was calculated. For the climatic factors, the mean annual temperature
195 (MAT), mean annual precipitation (MAP), isothermality, precipitation seasonality, and
196 temperature seasonality were compiled from the WorldClim version 2
197 (<https://www.worldclim.org/>) at 30 arc-second resolutions. Aridity index and potential
198 evapotranspiration (PET) were obtained from Global Aridity Index and Potential
199 Evapotranspiration (ET0) Climate Database v2 (<https://cgiarcsi.community>),
200 respectively.

201

202 **2.3 Soil DNA extraction and high-throughput sequencing**

203 Soil DNA was extracted by using FastDNA SPIN Kit (MP Biomedicals, Santa Ana,
204 CA, USA), according to the manufacturer's instructions. Then, the quality and
205 quantity of the extracted DNA were checked by using NanoDrop2000
206 spectrophotometer (NanoDrop Tech, Wilmington, USA) and 1% agarose gel
207 electrophoresis, respectively. The V4-V5 region of the bacterial *16S rRNA* gene was
208 amplified using the primers 515F (5'-GTGCCAGCMGCCGCGG-3') and 907R (5'-
209 CCGTCAATTCMTTTRAGTTT-3'). PCR reactions were performed on ABI
210 GeneAmp® 9700 (ABI, Waltham, MA, USA). High-throughput sequencing was
211 performed on an Illumina MiSeq PE300 platform (Illumina, Inc., San Diego, CA,
212 USA). All the generated raw sequences have been deposited in the Genome Sequence
213 Archive in National Genomics Data Center, China National Center for
214 Bioinformation/Beijing Institute of Genomics, Chinese Academy of Sciences, under
215 the accession number of CRA005208 (<https://bigd.big.ac.cn/gsa/browse/CRA005208>).

216

217 **2.4 Bioinformatic analyses**

218 Raw reads were processed using the amplicon sequence variants (ASV) method by
219 Quantitative Insight into Microbial Ecology 2 (QIIME2) (Bolyen et al., 2019).

220 Sequences with poor-quality (read length < 200 bp or average quality score < 25)
221 were discarded (Ladau et al., 2018). Finally, a total of 23,508,265 sequences were
222 obtained. The clean sequences were denoised using the DADA2 pipeline (Callahan et
223 al., 2016), and generated a total of 49,497 ASVs. Representative sequences were used
224 to construct the phylogenetic tree and for species annotations. SILVA database
225 (<https://www.arb-silva.de/>) was applied to assign the taxonomy. All the soil samples
226 were rarefied to 28,759 sequences (minimum) per sample for downstream analyses.

227

228 **2.5 Co-occurrence network constructions**

229 All the 407 soil samples were used to construct the co-occurrence networks by using
230 the *WGCNA* package (Langfelder & Horvath, 2012). ASVs that occur in less than 5
231 soil samples were excluded (Gao et al., 2021), leaving a total of 5, 134 ASVs. The
232 pairwise Spearman correlations matrix among ASVs were calculated, and p values
233 were corrected using Benjamini Hochberg's correction (Benjamini et al., 2006).
234 Nodes with correlations greater than 0.5 and $p < 0.001$ were retained (Delgado-
235 Baquerizo et al., 2018). The networks were visualized using Gephi (version 0.9.2).
236 Then, the ecological modules within the network were identified in Gephi, and the
237 relative abundance of each ecological module was calculated by averaging the
238 standardized relative abundance (Z-score). Sub-networks were generated from the
239 original network by preserving the presented nodes and edges of the target samples.
240 The topological parameters of all the generated networks were calculated, including
241 betweenness centrality (the number of times a node acts as a bridge along the shortest
242 path between two other nodes), closeness centrality (the number of steps required to
243 access all other nodes from a given node), clustering coefficient (a ratio of the number
244 of links between the neighbors of a node, and the maximum number of links that
245 could possibly exist between its neighbors) and degree (number of edges connecting a
246 node to other nodes). The average degree (avgK), represents the average number of
247 edges per node, was used to describe the network complexity (Yao et al., 2014).

248 Natural connectivity provides a sensitive discrimination of network structural
249 robustness. Thus, network robustness was estimated by removing nodes in the static
250 network to assess how quickly the natural connectivity degraded (Peng & Wu, 2016;
251 Wu et al., 2010).

252

253 **2.6 Statistical analyses**

254 To explore the environmental variables affecting bacterial alpha diversity, the
255 importance of variables was analyzed using the partial correlations method (Kim,
256 2015). We identified the major environmental factors that influencing the taxa's
257 relative abundance (i.e., the top ten phyla and core species). Multiple linear
258 regressions were fitted separately between taxa's relative abundance and
259 environmental variables using the `lm` function. Backward stepwise regression was
260 then performed to filter variables using `stepAIC` in *MASS* package. For the optimal
261 model obtained, the contribution of the main environmental variables to the total
262 variance in taxa's relative abundance was assessed using the `calc.relimp` function in
263 *relaimpo* package. A classification of random forest model was used to identify
264 biomarkers between Mud and SA habitats on class level using the *randomForest*
265 package (Liaw & Wiener, 2002). Then, the accuracy of the classification model was
266 assessed by receiver operating characteristic (ROC) and the prediction of confusion
267 matrix. Those ASVs that occurring in more than 50% samples were defined as core
268 species for Mud and SA habitat, respectively. Covariate adjusted principal coordinates
269 analysis (aPCoA) was used to describe pairwise dissimilarity between samples based
270 on the Weighted Unifrac distance (Shi et al., 2020). Pairwise permutational
271 multivariate analysis of variance (PERMANOVA) was used to test the significance of
272 differences in bacterial communities between soil samples. To better understand the
273 biodiversity patterns and to explore their underlying mechanisms, compositional
274 dissimilarities (BDtotal) were divided into Repl (species replacement) and RichDiff
275 (difference in abundance) components using the *adespatial* package. Dissimilarity-

276 overlap curve (DOC) was used to test whether the underlying ecological dynamics of
277 microbiomes are universal across all communities or unique to individual
278 communities (Kalyuzhny & Shnerb, 2017). We used a variety of methods to explore
279 the role of environmental factors in influencing bacterial communities. Firstly, the
280 variation partitioning analysis (VPA) was performed to estimate the effects of space,
281 depth, climate and soil factors on bacterial community using the *vegan* package. Then,
282 Mantel and partial Mantel tests were applied to examine the relationships between
283 environmental variables and bacterial communities. Finally, these relationships were
284 tested by the multiple regression on distance matrices (MRM) using the *ecodist*
285 packages, after filtering the environmental variables with high multicollinearity
286 (Spearman $\rho^2 > 0.7$) (Wang et al., 2017). Fast expectation-maximization microbial
287 source tracking (FEAST) analysis was used to estimate the source proportion of
288 bacteria in SA soils that derived from Mud soils, and vice versa (Shenhav et al.,
289 2019). All analyses involving R software were performed under R version 4.0.5 (R
290 Core Team, 2018), unless otherwise stated.

291 Structural equation model (SEM) was used to evaluate the direct and indirect
292 effects of biotic (i.e., module abundance, bacterial richness, network complexity) and
293 abiotic factors (i.e., climatic factors, soil properties) on soil TC. The predicted causal
294 relationships of the SEM were constructed based on prior knowledge (Delgado-
295 Baquerizo et al., 2020). All the environmental variables were treated as independently
296 observed variables in the SEM, rather than latent variable. Prior to SEM analysis, the
297 multicollinearity of environmental variables was examined by using the *Hmisc*
298 package, and those variables with Spearman ρ^2 greater than 0.7 were removed. Then,
299 Random Forest analyses were performed to identify the key predictors that
300 influencing soil TC by using the *rfPermute* package. A 1,000 permutation was then
301 applied to compute the null distribution and calculate the *p* values. Since most of the
302 variables were not normally distributed, the bootstrapping method were used to
303 evaluate the probability that the path coefficients differed from zero (Delgado-

304 Baquerizo et al., 2017). Then, three indices were used to assess the SEM performance
305 (Schermelleh-Engel & Moosbrugger, 2003): (1) Chi-square (χ^2) test, a good fit is
306 defined as $0 \leq \chi^2/df$ (degree of freedom) ≤ 2 , and $0.05 < p \leq 1.00$; (2) Root mean
307 square error of approximation (RMSEA), in which a good fit is defined as $0 \leq$
308 $RMSEA \leq 0.05$; (3) Bollen-Stine bootstrap test, a good fit is defined as $0.10 <$ Bollen-
309 Stine bootstrap $p \leq 1.00$. The standardized total effect of each predictor on soil TC
310 was calculated. SEM analyses were performed in AMOS 21 (IBM SPSS Inc., Chicago,
311 IL, USA).

312

313 **3. Results**

314 **3.1 Plant invasions causes drastic changes in soil environments and on the** 315 **biodiversity and community composition of soil bacteriomes**

316 A total of 18 environmental variables were obtained, including 11 soil properties (i.e.,
317 pH, salinity) and 7 climatic factors (i.e., MAT, MAP) (Table S2). Results show that
318 environmental variables varied considerably among habitats, sites, and soil depths. SA
319 soils have higher EC, salinity, total nitrogen (TN), SOM and water content than that
320 of Mud soils, but lower pH values. We further showed that plant invasions cause
321 important homogenization in soil environments. In particular, we found that important
322 soil properties such as Eh, soil temperature, TC, TS, C/N, and water content had
323 smaller changes in environmental variability than those in Mud soils. Yet, Mud habitat
324 and SA habitat had similar levels of total carbon ($p = 0.08$) (Fig. 2a). Both in the Mud
325 and SA habitats, the soil carbon content had a distinct latitudinal distribution pattern,
326 showing the highest at approximate 34°N regions. Not only that, compared to SA
327 habitat, the soil carbon in Mud habitat exhibited a larger increase with increasing soil
328 depth and then a subsequent decrease (Fig. 2b). Compared to Mud habitat, carbon
329 accumulation in SA habitats was mainly between the soil surface and 60 cm below
330 ground.

331 We then investigated patterns in soil microbial diversity. We used richness

332 (observed ASVs) to present the taxonomic alpha diversity of bacteria. Richness ($p <$
333 0.05) were significantly higher in SA soils compared with Mud soils, but not for all
334 the sites (Fig. 3a, Table S3). In general, richness increased with latitude but decreased
335 with soil depths (Fig. 3b, Fig. S1). We analyzed soil properties against richness for
336 revealing the main predictors. Three-ways ANOVAs showed that richness was mainly
337 influenced by the sample site heterogeneity ($F = 42.37$, $p < 0.001$) (Table S4). Partial
338 correlations analyses suggested that soil properties, rather than climatic factors, were
339 the primary factors in influencing richness (Fig. 3c). Among all the environmental
340 variables, soil temperature was found to be the best predictor (Fig. S2, Table S5).
341 Binomial regressions showed that richness decreasing when soil temperature beyond
342 the optimum ranges (Fig. 3d).

343 Venn diagram showing the share and unique ASVs, with 15,259 ASVs and
344 24,591 ASVs unique to Mud and SA soils respectively (Fig. S3a). A total of 60 phyla
345 were identified from all the soil samples, and the most abundant phyla was
346 *Proteobacteria*, *Chloroflexi*, and *Epsilonbacteraeota*, and their relative abundances
347 varied considerably across different sites and depths (Fig S3b). Among the top ten
348 phyla, SA soils have significantly ($p < 0.05$) higher relative abundances of
349 *Bacteroidetes*, *Acidobacteria*, *Planctomycetes*, *Gemmatimonadetes*, *Nitrospirae*, and
350 *Latescibacteria* than Mud soils, while have lower *Epsilonbacteraeota* (Fig. 4a).
351 Distinct latitudinal distributions were observed for these phyla, and the measured
352 environmental variables could explain 21.43%-74.01% of the variations in their
353 relative abundances (Fig. 4b, Fig. S4).

354 We identified 72 classes as the biomarkers between Mud and SA soils (Fig. S5a).
355 Both the results of area under curve (AUC = 0.77) of ROC and prediction of
356 confusion matrix ($0.21 < \text{error} < 0.22$) suggested a high accuracy of the classification
357 model (Fig. S5b, Table S6). These biomarkers included *Spirochaetia*, *Phycisphaerae*,
358 *Clostridia*, and others (Fig. S5c). In addition, at the 50% occurrence threshold, we
359 identified 8 and 5 core ASVs for Mud and SA soils respectively (Fig. S6a). Among

360 these core ASVs, 7 out of 13 ASVs were belong to class *Campylobacteria*, and the
361 other 6 ASVs were belong to class *Gammaproteobacteria* (Table S7). Although these
362 core ASVs were present in the majority of soil samples, their relative abundances
363 were varied across different sites and showed a clear latitudinal pattern, which found
364 to be mainly influenced by environmental factors (Fig. S6b, c, Fig. S7).

365

366 **3.2 Biotic homogenization of soil bacterial communities by *S. alterniflora***

367 Our findings further revealed that plant invasions are associated with important
368 continental-scale homogenizations of the soil bacteriomes of coastlines. First, we
369 found significant ($pseudo-F = 8.54$, $p < 0.001$) differences in the soil bacterial
370 communities between Mud and SA habitats (Fig. 5a). PERMANOVA suggested that
371 soil bacterial communities were mainly influenced by the factor of sample sites
372 ($pseudo-F = 23.41$, $p < 0.001$), followed by depths ($pseudo-F = 8.84$, $p < 0.001$) and
373 habitats ($pseudo-F = 8.54$, $p < 0.001$) (Table S8). We then showed that, in general, soil
374 microbiomes in SA microhabitat support less variability (distance of each sample to
375 its central point) among bacterial communities than Mud soils, suggesting the biotic
376 homogenization of bacterial community in SA soils compare to Mud soils (Fig. 5b,
377 Fig. S8). A significant pattern of distance decay relationship (DDR) was observed,
378 with the slopes of DDR of the SA soils higher than that of Mud soils, suggesting
379 higher spatial turnover of bacterial community after plant invasion (Fig. 5c). Beta
380 diversity (represented by BD_{total}) includes two components: species replacement
381 (Repl) and change in abundance (RichDiff). Results showed that Repl dominated the
382 bacterial community variation, accounting for 80.85% and 79.17% for Mud and SA
383 soils respectively (Fig. S9). DOC analysis further revealed that these ecological
384 dynamics of bacterial communities were universal across metacommunities (Fig.
385 S10a). Microorganisms could spread from one habitat to another. We used FEAST
386 (source tracking) method to quantify this dispersal event, and found a higher
387 proportion of Mud was derived from SA than vice versa (Fig. S10b).

388 We then used multiple approaches to explore the environmental variables
389 influencing the bacterial community structure. Firstly, partial Mantel tests
390 demonstrated the critical role of soil properties and climatic factors in affecting
391 bacterial communities (Table S9), which were further confirmed by the VPA analyses
392 (Fig. S11a). Then, the relationships between bacterial communities and environmental
393 variables were tested by Mantel tests (Fig. S11b, Table S10). MRM method, an
394 extension of partial Mantel analysis which offers several advantages over partial
395 Mantel tests, were applied to explore the key predictors (Table S11, Fig. S12). MRM
396 revealed that TS and TN were the decisive factors in influencing bacterial
397 communities for Mud and SA soils, respectively.

398

399 **3.3 *S. alterniflora* invasion reduces the complexity and robustness of co-** 400 **occurrence networks**

401 Co-occurrence networks were used to identify soil bacterial taxa organized within
402 closely-linked ecological clusters. The network consists of 4,230 nodes and 41,506
403 edges, with a high number of major nodes belong to phylum of *Proteobacteria*
404 (51.49%), *Bacteroidetes* (17.02%), *Chloroflexi* (7.85%), and *Epsilonbacteraeota*
405 (6.93%) (Fig. S13a). There are many nodes clustered together (modules) in the
406 network, of which, there are 7 modules containing more than 300 nodes, namely
407 Modules #36 (14.96%), Modules #45 (10.47%), Modules #27 (9.57%), Modules #25
408 (9.27%), Modules #42 (7.75%), Modules #22 (7.71%), and Modules #37 (7.66%) (Fig.
409 6a, Fig. S13b). Each module contains a wide variety of bacterial taxa, among which
410 the more abundant class groups include *Campylobacteria*, *Deltaproteobacteria*, and
411 *Bacilli* (Fig. 6b). The relative abundance of these modules was significantly ($p < 0.05$)
412 higher in SA habitats than in Mud habitats, including Modules #22, Modules #42, and
413 Modules #45 (Fig. 6c). Network properties characterize the physical structure of the
414 network, and the Mud network has significantly ($p < 0.05$) higher closeness centrality
415 (Mud: 0.20; SA: 0.19) and degree (Mud: 19.27; SA: 17.50) than the SA network,

416 suggesting a more complex network of Mud habitat (Fig. S14a, b). In addition, the
417 natural connectivity of the network decreased sharply as the proportion of removed
418 nodes increases, but the slope of the decline of Mud network was lower than that of
419 the SA network, means a more stable network of the Mud network (Fig. 6d). In order
420 to understand the spatial distributions of the network, sub-networks were constructed,
421 and results showed that the network complexity increases with increasing latitude for
422 both Mud and SA soils (Fig. 6e, Fig. S14c).

423

424 **3.4 Associations between bacterial communities and soil carbon pools**

425 SEM analysis helps us to understand the relationships between soil bacterial
426 communities and soil TC, while considering a variety of biotic and abiotic factors
427 simultaneously. Based on the initial model (Fig. S15), a Random Forest analysis was
428 performed to identify the key environmental factors (Fig. S16). SEM results showed
429 that soil TC was regulated by a combination of environmental factors, of which, the
430 most important were soil properties and climatic factors (Fig. 7). Notably, bacterial
431 community also played an important role in influencing TC, in detail, TC was
432 significantly and positively correlated with avgK (path coefficient = 0.15 ***) and
433 module #45 (path coefficient = 0.15 ***), while significantly and negatively
434 correlated with module #36 (path coefficient = -0.35 ***). Not only that, the presence
435 of aboveground plants also has a positive effect on soil TC (Fig. 7a). By analyzing the
436 total effect of each predictor, we found that ST was the most important factor in
437 regulating soil TC (Fig. 7b). From the results of the linear regression analysis, the
438 slope of the correlation between module #45 and avgK and TC was reduced in SA
439 habitats compared to Mud habitats, implying that the role of these bacterial taxa in TC
440 accumulation was diminished (Fig. 7c). Overall, these results have revealed the strong
441 associations between bacterial communities and soil TC, and which were reduced
442 after plant invasion.

443

444 **4. Discussion**

445 **4.1 Continental-scale *S. alterniflora* invasion increases bacterial alpha diversity,** 446 **and induces biotic homogenization of soil bacterial communities**

447 Plant invasions are an important threat to local biodiversity conservation and
448 ecosystem maintenance in the context of global change (Bradley et al., 2010;
449 Theoharides & Dukes, 2007). In the last few decades, many studies have been
450 conducted focusing on the effects of SA invasion on plant communities and soil biotas
451 in coastal wetlands (Chen & Wen, 2021; Yang et al., 2016). However, most of the
452 previous studies focusing on soil communities have been carried out at a local scale.
453 Here, we present the first continental-scale study investigating the impacts of plant
454 invasions on soil microbiomes in blue carbon coastal ecosystems.

455 We found that SA invasion significantly ($p < 0.05$) increased bacterial alpha
456 diversity in Chinese coastal wetlands (Fig. 3). Our results were consistent with
457 previous local-scale studies which revealed that SA invaded into Mud soils was found
458 to strongly increase the bacterial alpha diversity, in Fujian coastlines of southeast
459 China (Chen & Wen, 2021; Liu et al., 2017) and in Jiangsu Yancheng Wetland
460 National Nature Reserve (Yang et al., 2019). However, studies with inconsistent
461 results also exist, Gao et al. (2019) found that the bacterial alpha diversity of SA soils
462 in the Zhangjiang River Estuary Mangrove National Natural Reserve was comparable
463 to that of the Mud soils. Previous studies were done at a local scale, often impacted by
464 local environmental contexts, and difficult to interpret at a larger spatial scale
465 covering contrasting soil and climatic conditions. Unlike for those previous local
466 studies, our standardized continental survey aimed to capture the environmental
467 heterogeneity supporting the invasion of plants and their impacts on soil microbiomes.
468 Here, we provide continental-scale evidences that plant invasions can promote soil
469 bacterial diversity at the scale of China by introducing new species not previously
470 present in Mud soils, because plant colonization may provide resources and ecological
471 niches for the rare biosphere (Chen et al., 2019; Saleem et al., 2016). For instance,

472 Venn diagrams showed the share and unique ASVs, with 15,259 ASVs and 24,591
473 ASVs unique to Mud and SA soils respectively (Fig. S3a). These results suggest that
474 plant invasions can have a previously unreported impact on soil biodiversity, as
475 previously found for plant and animal diversity.

476 We further provided unprecedented evidences that continental-scale SA invasion
477 in China can cause important biotic homogenization of soil bacterial community (Fig.
478 5a, b, Fig. S8). Biotic homogenization following biological invasions is commonly
479 found for aboveground biodiversity (Stotz et al., 2019). For example, it has been
480 shown in many studies that biological invasions could lead to biotic homogenization
481 across different ecosystems, for animals and plants (Delgado-Baquerizo et al., 2021;
482 Gossner et al., 2016; Leprieur et al., 2007; Zhang et al., 2019). However, much less
483 studied are the impacts of plant invasions on soil microbiomes. The occurrence of
484 biotic homogenization does not conflict with our earlier observation that SA invasions
485 increase alpha diversity, as increases in local alpha diversity are usually accomplished
486 at the expense of beta diversity (Whittaker, 1972). Biotic homogenization is a process
487 whereby some species in a community are replaced by other species (Olden et al.,
488 2004; Olden & Poff, 2003). The invasion of SA could lead to biotic homogenization
489 of soil microbial community by altering soil physic-chemical properties, making them
490 more homogenous. In addition, compared to SA habitats, the dominant original native
491 ecosystems (Mud soils) are not protected by any vegetation, and are more susceptible
492 to environmental disturbance, which may cause greater microbial fluctuations. Not
493 only that, but bacteria in SA soils appeared to have a greater dispersal capacity than
494 that in Mud soils, as indicated by the results of source tracking (Fig. S10b), which
495 may favor biotic homogenization within the habitats. As a result, biotic
496 homogenization causes a narrowing of ecological niches within the community,
497 making microbes more responsive to environmental change and thus accelerating the
498 spatial turnover of the bacterial community (Fig. 5c). However, it is currently unclear
499 whether biotic homogenization also occurs at the genetic and functional levels

500 following SA invasion, beyond the taxonomic level. It has been shown that biotic
501 homogenization appears to reduce the multifunctionality in forest ecosystems (Van
502 Der Plas et al., 2016). Therefore, we speculate that SA invasion along the coastline in
503 China may impose strong influences on the microbial communities and the
504 biogeochemical cycles they support, and allow for the weakening or even loss of
505 certain ecological functions. Such changes would threaten the critical role of coastal
506 wetland ecosystems in global carbon cycling and climate change regulation.

507

508 **4.2 *S. alterniflora* invasion reduces the complexity and robustness of co-** 509 **occurrence networks**

510 Soils are home to hundreds of millions of microorganisms interacting with each other
511 and driving the fundamental soil processes (Faust & Raes, 2012; Layeghifard et al.,
512 2017). Dissecting the structure of soil microbial coexistence is important for a deeper
513 understanding of the evolution of soil ecological functions in response to
514 environmental changes. The impact of plant invasion on soil microbial networks has
515 mostly been studied at the local scale, but works at large spatial scales (i.e.,
516 continental scale) is still lacking (Chen & Wen, 2021; Zhang et al., 2020). Here, we
517 found that the continental-scale SA invasion causes a significant reduction in
518 connectivity between nodes within network and a consequent reduction in network
519 stability (Fig. 6, Fig. S14). Our study was consistent with that of others who also
520 found a decrease in network complexity of fungal communities after SA invasions in
521 a salt marsh ecosystem (Zhang et al., 2021). On the contrary, previous study reported
522 that SA invasion enhanced the bacterial interactions in the Yellow River Estuary of
523 China (Zhang et al., 2020). There are several reasons that may be used to support our
524 findings. Firstly, the biotic homogenization after SA invasion can be used to explain
525 the reduction in network complexity and stability, because microorganisms within a
526 community become more similar when biotic homogenization occurs and would
527 outcompete for similar resources, resulting in increased competition within the

528 community (Olden et al., 2004). Secondly, SA invasion strongly altered soil physico-
529 chemical properties, and this drastic environmental change exerts a strong selection
530 pressure on the soil bacterial community, thus excluding more microorganisms from
531 the network and leading to a simpler network (Ratzke et al., 2020). This seems to be
532 supported elsewhere by the fact that as the environment changed, more
533 microorganisms were replaced following the SA invasion (Fig. S9). Thirdly, high
534 diversity was accompanied by low network complexity. Within a community,
535 microorganisms can influence each other through competition, mutualism, predation,
536 and other actions (Faust & Raes, 2012). A community with high diversity means that
537 the habitat retains a greater diversity of microbial taxa that could compete for the
538 same type of resource, thus making the network become less complex (Farrer et al.,
539 2019). The reduced strength of the interactions between microorganisms leads to a
540 more unstable network which, if it collapses, will make it difficult to recover and
541 maintain normal ecological functioning (Olesen et al., 2007).

542

543 **4.3 Changes in the soil bacteriome are associated with those in carbon pools**

544 Coastal wetlands are important blue carbon ecosystems on Earth, with stronger carbon
545 sequestration than other biomes (Alongi, 2014). Given such a large soil carbon pool in
546 coastal wetland soils, it's subtle changes may have important implications for global
547 climate change. Therefore, it is ecologically important to explore the coupling
548 relationship between soil microbiome and carbon pools, as microorganisms play key
549 roles in mediating the carbon dynamic. In this study, we provided evidence that
550 multiple environmental factors jointly regulate soil total carbon (Fig. 7). Soil TC was
551 increased after SA invasion (Fig. 2), and this positive effects of SA on soil TC have
552 been extensively verified in previous studies (Barry et al., 2021; Li et al., 2020; Zhang
553 et al., 2021). Noteworthy, a positive association between network complexity and TC
554 was found. A community with high network complexity implies that microorganisms
555 within the community are more closely linked. The existence of complementarity

556 effects between microorganisms, as when species use differentiated resources they are
557 more likely to co-exist within a community, leading to complementarity effects and
558 positively contributing to ecological functions (Godoy et al., 2020; Turnbull et al.,
559 2016).

560 In addition, the relationship between microbes and soil TC was weakened after
561 SA invasion (Fig. 7c). SA, C4 perennial herb, has a strong carbon sequestration
562 capacity and can allocate the fixed carbon to the soil through root exudations and litter
563 input. Although SA invasion significantly impacting the modularity of ecological
564 networks influencing the relative abundance of specific microbial modules including
565 multiple soil individual taxa (Fig. 6c). The positive influence of SA on organic carbon
566 is likely to disconnect the multiple microbial metabolic connections needed to extract
567 carbon resources in low carbon ecosystems, favoring the proportion of certain
568 microbial individual taxa (microbial modules within the ecological network) over
569 others. The disconnection between carbon and soil microbial communities associated
570 with plant invasions still have unknown consequences for the environment, yet
571 increase the uncertainty on the capacity of carbon blue ecosystems to regulate global
572 carbon cycling compared with native environments. Currently, many countries are
573 actively promoting efforts to achieve carbon neutrality goals. Given the excellent
574 carbon sink capacity of coastal wetlands, the decoupling of soil microorganisms and
575 carbon pools after SA invasion may limit the potential of microorganisms in balancing
576 carbon sink and source.

577

578 **5. Conclusions**

579 Our work provides the first continental-scale evidence of the impacts of plant
580 invasions on soil microbiomes. We show the biogeography of soil bacterial
581 communities following continental-scale plant invasions, considering diversity,
582 community structure, co-occurrence network and link with function. Plant invasion
583 dramatically increased bacterial alpha diversity, while decreased the complexity and

584 robustness of the co-occurrence networks. Plant invasion also caused significant
585 biotic homogenization, and weakened the role of microbes in mediating soil TC
586 accumulation. Overall, these findings have broadened our knowledge on the soil
587 bacterial biogeography following plant invasion in Chinese coastal wetlands, which
588 helps to understand their compositional and functional dynamic under global change.

589

590 **Acknowledgements**

591 This study was financially supported by the National Natural Science Foundation of
592 China (41907040, 91951109), the National Key Research and Development Program
593 of China (2017YFC0506102), and the Jiangsu Planned Projects for Postdoctoral
594 Research Funds (2019Z394). M.D-B. is supported by a project from the Spanish
595 Ministry of Science and Innovation (PID2020-115813RA-I00), and a project of the
596 Fondo Europeo de Desarrollo Regional (FEDER) and the Consejería de
597 Transformación Económica, Industria, Conocimiento y Universidades of the Junta de
598 Andalucía (FEDER Andalucía 2014-2020 Objetivo temático “01 - Refuerzo de la
599 investigación, el desarrollo tecnológico y la innovación”) associated with the research
600 project P20_00879 (ANDABIOMA). We are grateful to the anonymous reviewers for
601 their constructive comments and suggestions, which greatly improved the manuscript.

602

603 **Conflict of interest**

604 The authors declare that they have no conflict of interest.

605

606 **Data availability statement**

607 The data that support the findings of this study are openly available in figshare at
608 <https://doi.org/10.6084/m9.figshare.19534285.v4>

609

610 **Figure legends**

611 **Fig. 1|** The sample sites and their corresponding MAT along the coastal wetlands in

612 China (a). The locations of each replicate in a 50*50 m quadrat for Mud and SA
613 habitats. Five intact soil cores were randomly collected and completely mixed as a
614 replicate (b). Schematic diagram of the sampling depth for each sample site (c). Mud:
615 bare mudflat; SA: *Spartina alterniflora*; HLD: Huludao; TG: Tanggu; DY: Dongying;
616 LYG: Lianyungang; YC: Yancheng; CM: Chongming; YQ: Yueqing; XP: Xiapu; YX:
617 Yunxiao; ZH: Zhuhai; BH: Beihai; ZJ: Zhanjiang; MAT: mean annual temperature.

618

619 **Fig. 2**| Soil total carbon (TC) content in coastal wetlands. The latitudinal pattern of
620 soil TC for Mud and SA habitats respectively (a). Variation of soil TC with depth (b).

621 For abbreviations, see the legends of Fig. 1.

622

623 **Fig. 3**| The influence of plant invasions on the response of bacterial richness to
624 environmental variability. Difference in bacterial richness between Mud and SA
625 habitats, and the significance was examined by Wilcoxon rank sum test (a). Variations
626 of bacterial richness in various depths (b). Partial Spearman correlations between
627 bacterial richness and the groups of environmental variables (i.e., space, climate,
628 habitat, depth and soil) (c). All observed variables were grouped into corresponding
629 groups and constructed as latent variables. Latent variables were constructed using the
630 Partial Least Squares Path Modeling (PLS-PM) method. The relationships between
631 richness and soil temperature (d). Both linear and quadratic models were used to fit
632 these relationships, and best models were selected based on a low Akaike's
633 information criterion (AIC) value. * $p < 0.05$; ** $p < 0.01$; *** $p < 0.001$. For
634 abbreviations, see the legends of Fig. 1.

635

636 **Fig. 4**| The relative abundance of the bacterial top ten phyla. Differences in the
637 relative abundance of the top ten bacterial phyla between Mud and SA habitats (a).
638 Trends in the relative abundance of the top ten bacterial phyla with latitude (b). * $p <$
639 0.05 ; ** $p < 0.01$; *** $p < 0.001$. For abbreviations, see the legends of Fig. 1.

640

641 **Fig. 5**| The influence of plant invasions on bacterial community composition and
642 heterogeneity. Results of the covariate adjusted principal coordinates analysis (aPCoA)
643 based on the Weighted UniFrac distance revealing the pairwise dissimilarities
644 between Mud and SA habitats. The significant differences were examined by pairwise
645 permutational multivariate analysis of variance (PERMANOVA) tests (a). Distance of
646 soil bacterial community to centroid point within each sample site (b). Distance decay
647 relationship reveals the relationship between bacterial community similarity and
648 geographical distance (c). The solid and dashed lines indicate significant and
649 insignificant relationships, respectively. * $p < 0.05$; ** $p < 0.01$; *** $p < 0.001$. For
650 abbreviations, see the legends of Fig. 1.

651

652 **Fig. 6**| The influence of plant invasions on soil ecological networks. Modules (groups
653 of taxa highly co-occurring with each other) with >300 taxa (nodes) within the
654 ecological network (a). The community composition for the top microbial modules (b).
655 The difference in the relative abundance of each ecological module between Mud and
656 SA habitats, and significance was tested by Wilcoxon test (c). The network structural
657 robustness assessed by the decline in natural connectivity against the removing nodes
658 (d). The higher the slope represents the more drastic the decline in network structural
659 robustness, in other words, the more unstable the network is. The latitudinal pattern of
660 the network's average degree (avgK), representing the network complexity (e). * $p <$
661 0.05 ; ** $p < 0.01$; *** $p < 0.001$. For abbreviations, see the legends of Fig. 1.

662

663 **Fig. 7**| Structural equation model (SEM) revealing the direct and indirect effects of
664 environmental variables on soil TC (a). To obtain a simplified graphic, different
665 blocks were used to represent the various types of environmental factors, but note that
666 all variables were treated as observed variables. Numbers within parentheses are the
667 path coefficients and are indicative of the standardized effect size of the relationship.

668 Solid and dashed arrows indicate positive and negative effects, respectively. R^2 value
669 means the proportion of variance explained. The standardized total effects of each
670 predictor attributes on soil TC (b). The relationships between soil TC and bacterial
671 communities (Mod #36, Mod #45, and avgK) (c). Solid and dashed lines indicate
672 significant and insignificant correlations, respectively. Long: longitude; Lat: latitude;
673 Mod: module; Iso: isothermality; MAP: mean annual precipitation; PET: potential
674 evapotranspiration; avgK: average degree; ST: soil temperature; TN: total nitrogen;
675 TC: total carbon. * $p < 0.05$; ** $p < 0.01$; *** $p < 0.001$. For abbreviations, see the
676 legends of Fig. 1.

677 **References**

- 678 Alongi, D. M. (2014). Carbon cycling and storage in mangrove forests. *Annual*
679 *Review of Marine Science*, 6(1), 195–219. [https://doi.org/10.1146/annurev-](https://doi.org/10.1146/annurev-marine-010213-135020)
680 [marine-010213-135020](https://doi.org/10.1146/annurev-marine-010213-135020)
- 681 An, S. Q., Gu, B. H., Zhou, C. F., Wang, Z. S., Deng, Z. F., Zhi, Y. B., Li, H. L.,
682 Chen, L., Yu, D. H., & Liu, Y. H. (2007). *Spartina* invasion in China:
683 Implications for invasive species management and future research. *Weed*
684 *Research*, 47(3), 183–191. <https://doi.org/10.1111/j.1365-3180.2007.00559.x>
- 685 Barry, A., Ooi, S. K., Helton, A. M., Steven, B., Elphick, C. S., & Lawrence, B. A.
686 (2021). Vegetation zonation predicts soil carbon mineralization and microbial
687 communities in Southern New England salt marshes. *Estuaries and Coasts*, 45,
688 168–180. <https://doi.org/10.1007/s12237-021-00943-0>
- 689 Benjamini, Y., Krieger, A. M., & Yekutieli, D. (2006). Adaptive linear step-up
690 procedures that control the false discovery rate. *Biometrika*, 93(3), 491–507.
691 <https://doi.org/10.1093/biomet/93.3.491>
- 692 Bolyen, E., Rideout, J. R., Dillon, M. R., Bokulich, N. A., Abnet, C. C., Al-Ghalith, G.
693 A., Alexander, H., Alm, E. J., Arumugam, M., Asnicar, F., Bai, Y., Bisanz, J. E.,
694 Bittinger, K., Brejnrod, A., Brislawn, C. J., Brown, C. T., Callahan, B. J.,
695 Caraballo-Rodríguez, A. M., Chase, J., ... Caporaso, J. G. (2019). Reproducible,
696 interactive, scalable and extensible microbiome data science using QIIME 2.
697 *Nature Biotechnology*, 37, 852–857. <https://doi.org/10.1038/s41587-019-0209-9>
- 698 Bradley, B. A., Blumenthal, D. M., Wilcove, D. S., & Ziska, L. H. (2010). Predicting
699 plant invasions in an era of global change. *Trends in Ecology & Evolution*, 25(5),
700 310–318. <https://doi.org/10.1016/j.tree.2009.12.003>
- 701 Callahan, B. J., McMurdie, P. J., Rosen, M. J., Han, A. W., Johnson, A. J. A., &
702 Holmes, S. P. (2016). DADA2: High-resolution sample inference from Illumina
703 amplicon data. *Nature Methods*, 13(7), 581–583.
704 <https://doi.org/10.1038/nmeth.3869>

705 Chen, L., Fang, K., Zhou, J., Yang, Z. P., Dong, X. F., Dai, G. H., & Zhang, H. B.
706 (2019). Enrichment of soil rare bacteria in root by an invasive plant *Ageratina*
707 *adenophora*. *Science of the Total Environment*, 683, 202–209.
708 <https://doi.org/10.1016/j.scitotenv.2019.05.220>

709 Chen, W., & Wen, D. (2021). Archaeal and bacterial communities assembly and co-
710 occurrence networks in subtropical mangrove sediments under *Spartina*
711 *alterniflora* invasion. *Environmental Microbiome*, 16, 10.
712 <https://doi.org/10.1186/s40793-021-00377-y>

713 Chen, Z., Li, B., Zhong, Y., & Chen, J. (2004). Local competitive effects of
714 introduced *Spartina alterniflora* on *Scirpus mariqueter* at Dongtan of
715 Chongming Island, the Yangtze River estuary and their potential ecological
716 consequences. *Hydrobiologia*, 528, 99–106. [https://doi.org/10.1007/s10750-004-](https://doi.org/10.1007/s10750-004-1888-9)
717 1888-9

718 Delgado-Baquerizo, M., Eldridge, D. J., Liu, Y.-R., Sokoya, B., Wang, J.-T., Hu, H.-
719 W., He, J.-Z., Bastida, F., Moreno, J. L., Bamigboye, A. R., Blanco-Pastor, J. L.,
720 Cano-Díaz, C., Illán, J. G., Makhalanyane, T. P., Siebe, C., Trivedi, P., Zaady, E.,
721 Verma, J. P., Wang, L., ... Fierer, N. (2021). Global homogenization of the
722 structure and function in the soil microbiome of urban greenspaces. *Science*
723 *Advances*, 7(28), eabg5809. <https://doi.org/10.1126/sciadv.abg5809>

724 Delgado-Baquerizo, M., Eldridge, D. J., Ochoa, V., Gozalo, B., Singh, B. K., &
725 Maestre, F. T. (2017). Soil microbial communities drive the resistance of
726 ecosystem multifunctionality to global change in drylands across the globe.
727 *Ecology Letters*, 20(10), 1295–1305. <https://doi.org/10.1111/ele.12826>

728 Delgado-Baquerizo, M., Reich, P. B., Trivedi, C., Eldridge, D. J., Abades, S., Alfaro,
729 F. D., Bastida, F., Berhe, A. A., Cutler, N. A., Gallardo, A., García-Velázquez,
730 L., Hart, S. C., Hayes, P. E., He, J.-Z., Hseu, Z.-Y., Hu, H.-W., Kirchmair, M.,
731 Neuhauser, S., Pérez, C. A., ... Singh, B. K. (2020). Multiple elements of soil
732 biodiversity drive ecosystem functions across biomes. *Nature Ecology &*

733 *Evolution*, 4, 210–220. <https://doi.org/10.1038/s41559-019-1084-y>

734 Delgado-Baquerizo, M., Reith, F., Dennis, P. G., Hamonts, K., Powell, J. R., Young,
735 A., Singh, B. K., & Bissett, A. (2018). Ecological drivers of soil microbial
736 diversity and soil biological networks in the Southern Hemisphere. *Ecology*,
737 99(3), 583–596. <https://doi.org/10.1002/ecy.2137>

738 Farrer, E. C., Porazinska, D. L., Spasojevic, M. J., King, A. J., Bueno de Mesquita, C.
739 P., Sartwell, S. A., Smith, J. G., White, C. T., Schmidt, S. K., & Suding, K. N.
740 (2019). Soil microbial networks shift across a high-elevation successional
741 gradient. *Frontiers in Microbiology*, 10, 2887.
742 <https://doi.org/10.3389/fmicb.2019.02887>

743 Faust, K., & Raes, J. (2012). Microbial interactions: From networks to models. *Nature*
744 *Reviews Microbiology*, 10, 538–550. <https://doi.org/10.1038/nrmicro2832>

745 Gao, G.-F., Li, P.-F., Zhong, J.-X., Shen, Z.-J., Chen, J., Li, Y.-T., Isabwe, A., Zhu,
746 X.-Y., Ding, Q.-S., Zhang, S., Gao, C.-H., & Zheng, H.-L. (2019). *Spartina*
747 *alterniflora* invasion alters soil bacterial communities and enhances soil N₂O
748 emissions by stimulating soil denitrification in mangrove wetland. *Science of The*
749 *Total Environment*, 653, 231–240.
750 <https://doi.org/10.1016/j.scitotenv.2018.10.277>

751 Gao, G.-F., Li, H., Shi, Y., Yang, T., Gao, C.-H., Fan, K., Zhang, Y., Zhu Y.-G.,
752 Delgado-Baquerizo M., Zheng, H.-L., & Chu, H. (2022). Metadata of soils in
753 *Spartina alterniflora* salt marshes and their adjacent mudflats along coastlines of
754 China. figshare. Dataset. <https://doi.org/10.6084/m9.figshare.19534285.v4>

755 Gao, G.-F., Peng, D., Wu, D., Zhang, Y., & Chu, H. (2021). Increasing inundation
756 frequencies enhance the stochastic process and network complexity of soil
757 archaeal community in coastal wetlands. *Applied and Environmental*
758 *Microbiology*, 87(11), e02560-20. <https://doi.org/10.1128/AEM.02560-20>

759 Godoy, O., Gómez-Aparicio, L., Matías, L., Pérez-Ramos, I. M., & Allan, E. (2020).
760 An excess of niche differences maximizes ecosystem functioning. *Nature*

761 *Communications*, 11, 4180. <https://doi.org/10.1038/s41467-020-17960-5>

762 Gossner, M. M., Lewinsohn, T. M., Kahl, T., Grassein, F., Boch, S., Prati, D.,
763 Birkhofer, K., Renner, S. C., Sikorski, J., Wubet, T., Arndt, H., Baumgartner, V.,
764 Blaser, S., Blüthgen, N., Börschig, C., Buscot, F., Diekötter, T., Jorge, L. R.,
765 Jung, K., ... Allan, E. (2016). Land-use intensification causes multitrophic
766 homogenization of grassland communities. *Nature*, 540, 266–269.
767 <https://doi.org/10.1038/nature20575>

768 He, W., Feagin, R., Lu, J., Liu, W., Yan, Q., & Xie, Z. (2007). Impacts of introduced
769 *Spartina alterniflora* along an elevation gradient at the Jiuduansha Shoals in the
770 Yangtze Estuary, suburban Shanghai, China. *Ecological Engineering*, 29(3),
771 245–248. <https://doi.org/10.1016/j.ecoleng.2006.08.004>

772 Heiri, O., Lotter, A. F., Lemcke, G., André F. Lotter, & Gerry Lemcke. (2001). Loss
773 on ignition as a method for estimating organic and carbonate content in
774 sediments: Reproducibility and comparability of results. *Journal of*
775 *Paleolimnology*, 25, 101–110. <https://doi.org/10.1023/A:1008119611481>

776 Kalyuzhny, M., & Shnerb, N. M. (2017). Dissimilarity-overlap analysis of community
777 dynamics: Opportunities and pitfalls. *Methods in Ecology and Evolution*, 8(12),
778 1764–1773. <https://doi.org/10.1111/2041-210X.12809>

779 Kim, S. (2015). ppcor: An R package for a fast calculation to semi-partial correlation
780 coefficients. *Communications for Statistical Applications and Methods*, 22(6),
781 665–674. <https://doi.org/10.5351/csam.2015.22.6.665>

782 Ladau, J., Shi, Y., Jing, X., He, J.-S., Chen, L., Lin, X., Fierer, N., Gilbert, J. A.,
783 Pollard, K. S., & Chu, H. (2018). Existing climate change will lead to
784 pronounced shifts in the diversity of soil prokaryotes. *mSystems*, 3(5), e00167-18.
785 <https://doi.org/10.1128/mSystems.00167-18>

786 Langfelder, P., & Horvath, S. (2012). Fast R functions for robust correlations and
787 hierarchical clustering. *Journal of Statistical Software*, 46(11), 1–17.
788 <https://doi.org/10.18637/jss.v046.i11>

789 Layeghifard, M., Hwang, D. M., & Guttman, D. S. (2017). Disentangling interactions
790 in the microbiome: A network perspective. *Trends in Microbiology*, 25(3), 217–
791 228. <https://doi.org/10.1016/j.tim.2016.11.008>

792 Leprieur, F., Beauchard, O., Hugueny, B., Grenouillet, G., & Brosse, S. (2007). Null
793 model of biotic homogenization: A test with the European freshwater fish fauna.
794 *Diversity and Distributions*, 14(2), 291–300. [https://doi.org/10.1111/j.1472-](https://doi.org/10.1111/j.1472-4642.2007.00409.x)
795 [4642.2007.00409.x](https://doi.org/10.1111/j.1472-4642.2007.00409.x)

796 Li, Y. X., Laborda, P., Xie, X. L., Zhou, R., Chen, Y., Li, T., Pu, Z. H., Wang, Y. L.,
797 & Deng, Z. F. (2020). *Spartina alterniflora* invasion alters soil microbial
798 metabolism in coastal wetland of China. *Estuarine, Coastal and Shelf Science*,
799 245, 106982. <https://doi.org/10.1016/j.ecss.2020.106982>

800 Liaw, A., & Wiener, M. (2002). Classification and regression by randomForest. *R*
801 *News*, 2, 18–22.

802 Liu, M., Mao, D., Wang, Z., Li, L., Man, W., Jia, M., Ren, C., & Zhang, Y. (2018).
803 Rapid invasion of *Spartina alterniflora* in the coastal zone of Mainland China:
804 New observations from Landsat OLI images. *Remote Sensing*, 10(12), 1933.
805 <https://doi.org/10.3390/rs10121933>

806 Liu, M., Yu, Z., Yu, X., Xue, Y., Huang, B., & Yang, J. (2017). Invasion by cordgrass
807 increases microbial diversity and alters community composition in a mangrove
808 nature reserve. *Frontiers in Microbiology*, 8, 2503.
809 <https://doi.org/10.3389/fmicb.2017.02503>

810 Muthukrishnan, R., & Larkin, D. J. (2020). Invasive species and biotic
811 homogenization in temperate aquatic plant communities. *Global Ecology and*
812 *Biogeography*, 29(4), 656–667. <https://doi.org/10.1111/geb.13053>

813 Olden, J. D., & Poff, N. L. (2004). Ecological processes driving biotic
814 homogenization: Testing a mechanistic model using fish faunas. *Ecology*, 85(7),
815 1867–1875. <https://doi.org/10.1890/03-3131>

816 Olden, J. D., & Poff, N. L. R. (2003). Toward a mechanistic understanding and

817 prediction of biotic homogenization. *American Naturalist*, 162(4), 442–460.
818 <https://doi.org/10.1086/378212>

819 Olden, J. D., Poff, N. L. R., Douglas, M. R., Douglas, M. E., & Fausch, K. D. (2004).
820 Ecological and evolutionary consequences of biotic homogenization. *Trends in*
821 *Ecology and Evolution*, 19(1), 18–24. <https://doi.org/10.1016/j.tree.2003.09.010>

822 Olesen, J. M., Bascompte, J., Dupont, Y. L., & Jordano, P. (2007). The modularity of
823 pollination networks. *Proceedings of the National Academy of Sciences of the*
824 *United States of America*, 104(50), 19891–19896.
825 <https://doi.org/10.1073/pnas.0706375104>

826 Osland, M. J., Enwright, N. M., Day, R. H., Gabler, C. A., Stagg, C. L., & Grace, J. B.
827 (2016). Beyond just sea-level rise: Considering macroclimatic drivers within
828 coastal wetland vulnerability assessments to climate change. *Global Change*
829 *Biology*, 22(1), 1–11. <https://doi.org/10.1111/gcb.13084>

830 Peng, G. S., & Wu, J. (2016). Optimal network topology for structural robustness
831 based on natural connectivity. *Physica A: Statistical Mechanics and Its*
832 *Applications*, 443, 212–220. <https://doi.org/10.1016/j.physa.2015.09.023>

833 R Core Team. (2018). A language and environment for statistical computing. R
834 Foundation for Statistical Computing, Vienna, Austria.

835 Ratzke, C., Barrere, J., & Gore, J. (2020). Strength of species interactions determines
836 biodiversity and stability in microbial communities. *Nature Ecology & Evolution*,
837 4, 376–383. <https://doi.org/10.1038/s41559-020-1099-4>

838 Saleem, M., Law, A. D., & Moe, L. A. (2016). *Nicotiana* roots recruit rare
839 rhizosphere taxa as major root-inhabiting microbes. *Microbial Ecology*, 71, 469–
840 472. <https://doi.org/10.1007/s00248-015-0672-x>

841 Schermelleh-Engel, K., & Moosbrugger, H. (2003). Evaluating the fit of structural
842 equation models: Tests of significance and descriptive goodness-of-fit measures.
843 *Methods of Psychological Research Online*, 8(2), 23–74.

844 Schuerch, M., Spencer, T., Temmerman, S., Kirwan, M. L., Wolff, C., Lincke, D.,

845 McOwen, C. J., Pickering, M. D., Reef, R., Vafeidis, A. T., Hinkel, J., Nicholls,
846 R. J., & Brown, S. (2018). Future response of global coastal wetlands to sea-
847 level rise. *Nature*, *561*, 231–234. <https://doi.org/10.1038/s41586-018-0476-5>

848 Shenhav, L., Thompson, M., Joseph, T. A., Briscoe, L., Furman, O., Bogumil, D.,
849 Mizrahi, I., Pe'er, I., & Halperin, E. (2019). FEAST: Fast expectation-
850 maximization for microbial source tracking. *Nature Methods*, *16*, 627–632.
851 <https://doi.org/10.1038/s41592-019-0431-x>

852 Shi, Y., Zhang, L., Do, K.-A., Peterson, C. B., & Jenq, R. R. (2020). aPCoA:
853 Covariate adjusted principal coordinates analysis. *Bioinformatics*, *36*(13), 4099–
854 4101. <https://doi.org/10.1093/bioinformatics/btaa276>

855 Stotz, G. C., Gianoli, E., & Cahill, J. F. (2019). Biotic homogenization within and
856 across eight widely distributed grasslands following invasion by *Bromus inermis*.
857 *Ecology*, *100*(7), e02717. <https://doi.org/10.1002/ecy.2717>

858 Theoharides, K. A., & Dukes, J. S. (2007). Plant invasion across space and time:
859 Factors affecting nonindigenous species success during four stages of invasion.
860 *New Phytologist*, *176*(2), 256–273. [https://doi.org/10.1111/j.1469-](https://doi.org/10.1111/j.1469-8137.2007.02207.x)
861 [8137.2007.02207.x](https://doi.org/10.1111/j.1469-8137.2007.02207.x)

862 Turnbull, L. A., Isbell, F., Purves, D. W., Loreau, M., & Hector, A. (2016).
863 Understanding the value of plant diversity for ecosystem functioning through
864 niche theory. *Proceedings of the Royal Society B: Biological Sciences*,
865 *283*(1844), 20160536. <https://doi.org/10.1098/rspb.2016.0536>

866 Van Der Plas, F., Manning, P., Soliveres, S., Allan, E., Scherer-Lorenzen, M.,
867 Verheyen, K., Wirth, C., Zavala, M. A., Ampoorter, E., Baeten, L., Barbaro, L.,
868 Bauhus, J., Benavides, R., Benneter, A., Bonal, D., Bouriaud, O., Bruelheide, H.,
869 Bussotti, F., Carnol, M., ... Fischer, M. (2016). Biotic homogenization can
870 decrease landscape-scale forest multifunctionality. *Proceedings of the National*
871 *Academy of Sciences of the United States of America*, *113*(13), E2549.
872 <https://doi.org/10.1073/pnas.1605668113>

873 Wang, X.-B., Lü, X.-T., Yao, J., Wang, Z.-W., Deng, Y., Cheng, W.-X., Zhou, J.-Z.,
874 & Han, X.-G. (2017). Habitat-specific patterns and drivers of bacterial β -
875 diversity in China's drylands. *The ISME Journal*, *11*, 1345–1358.
876 <https://doi.org/10.1038/ismej.2017.11>

877 Wang, X., Xiao, X., Zou, Z., Hou, L., Qin, Y., Dong, J., Doughty, R. B., Chen, B.,
878 Zhang, X., Chen, Y., Ma, J., Zhao, B., & Li, B. (2020). Mapping coastal
879 wetlands of China using time series Landsat images in 2018 and Google Earth
880 Engine. *ISPRS Journal of Photogrammetry and Remote Sensing*, *163*, 312–326.
881 <https://doi.org/10.1016/j.isprsjprs.2020.03.014>

882 Whittaker, R. H. (1972). Evolution and measurement of species. *Taxon*, *21*, 213–251.

883 Wu, J., Mauricio, B., Tan, Y.-J., & Deng, H.-Z. (2010). Natural connectivity of
884 complex networks. *Chinese Physics Letters*, *27*(7), 078902.
885 <https://doi.org/10.1088/0256-307X/27/7/078902>

886 Yang, W., Jeelani, N., Leng, X., Cheng, X. L., & An, S. Q. (2016). *Spartina*
887 *alterniflora* invasion alters soil microbial community composition and microbial
888 respiration following invasion chronosequence in a coastal wetland of China.
889 *Scientific Reports*, *6*, 26880. <https://doi.org/10.1038/srep26880>

890 Yang, W., Jeelani, N., Zhu, Z., Luo, Y., Cheng, X., & An, S. (2019). Alterations in
891 soil bacterial community in relation to *Spartina alterniflora* Loisel. invasion
892 chronosequence in the eastern Chinese coastal wetlands. *Applied Soil Ecology*,
893 *135*, 38–43. <https://doi.org/10.1016/j.apsoil.2018.11.009>

894 Yao, M., Rui, J., Li, J., Dai, Y., Bai, Y., Hed, P., Wang, J., Zhang, S., Pei, K., Liu, C.,
895 Wang, Y., He, Z., Frouz, J., Li, X., Heděnc, P., Wang, J., Zhang, S., Pei, K., Liu,
896 C., ... Li, X. (2014). Rate-specific responses of prokaryotic diversity and
897 structure to nitrogen deposition in the *Leymus chinensis* steppe. *Soil Biology and*
898 *Biochemistry*, *79*, 81–90. <https://doi.org/10.1016/j.soilbio.2014.09.009>

899 Zhang, G., Bai, J., Tebbe, C. C., Huang, L., Jia, J., Wang, W., Wang, X., Yu, L., &
900 Zhao, Q. (2021). *Spartina alterniflora* invasions reduce soil fungal diversity and

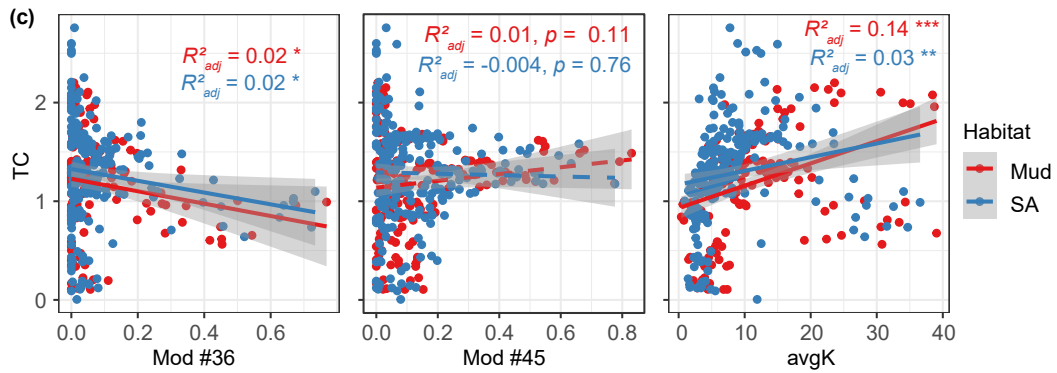
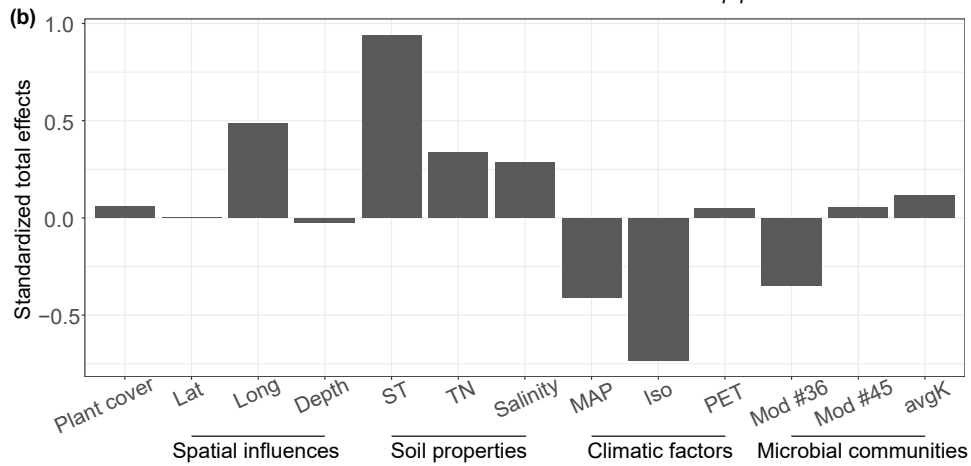
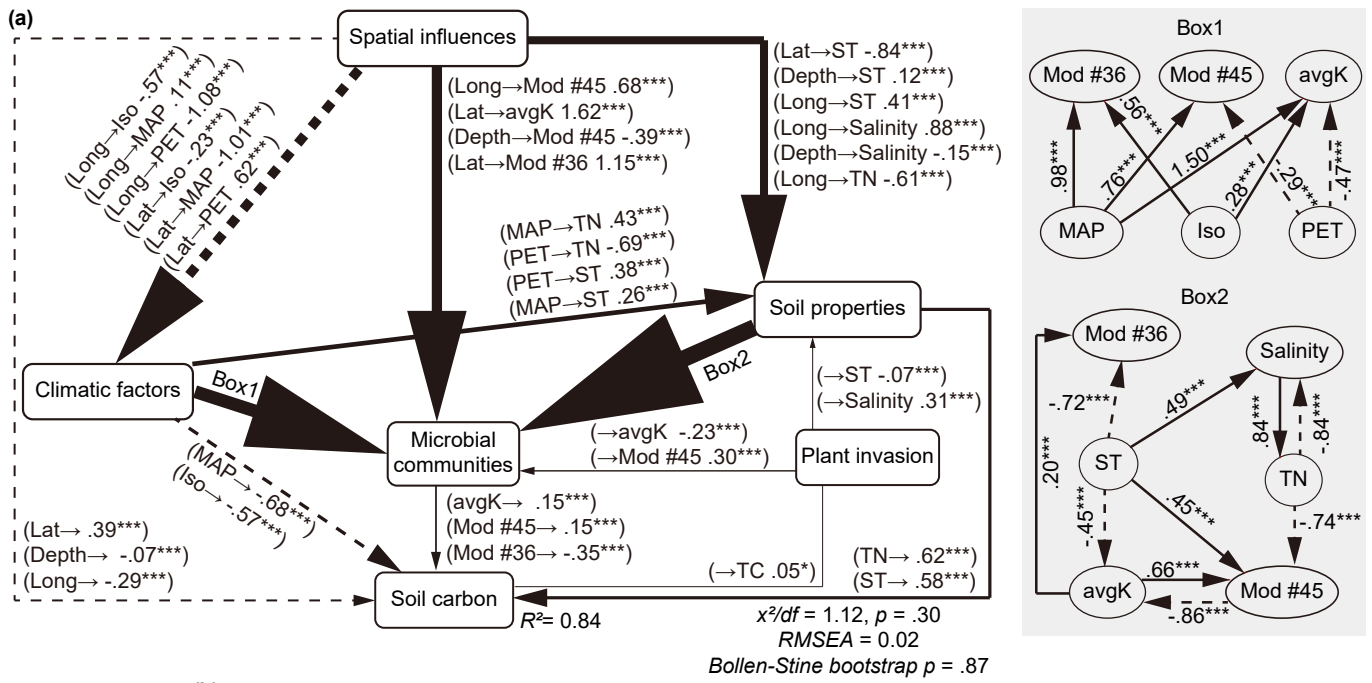
901 simplify co-occurrence networks in a salt marsh ecosystem. *Science of the Total*
902 *Environment*, 758, 143667. <https://doi.org/10.1016/j.scitotenv.2020.143667>

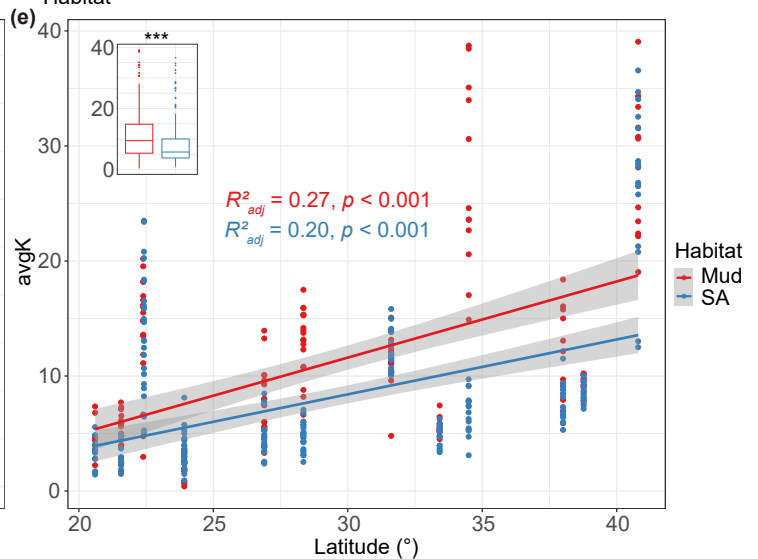
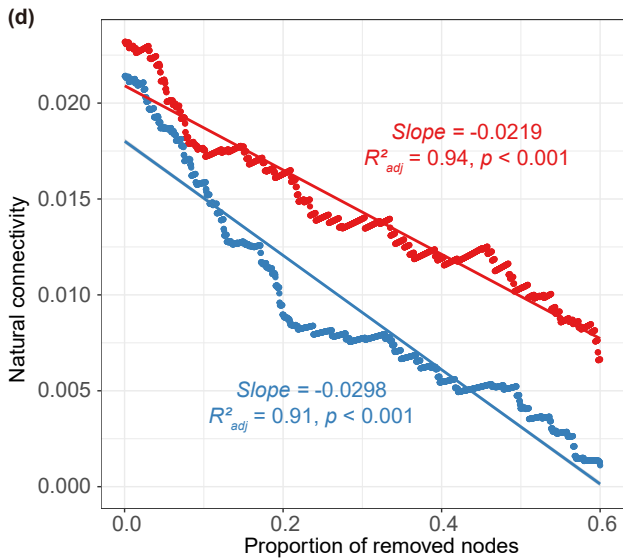
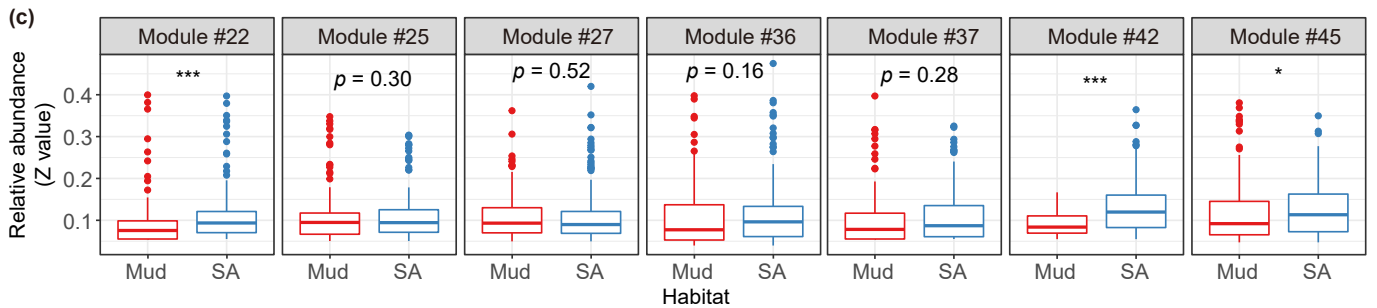
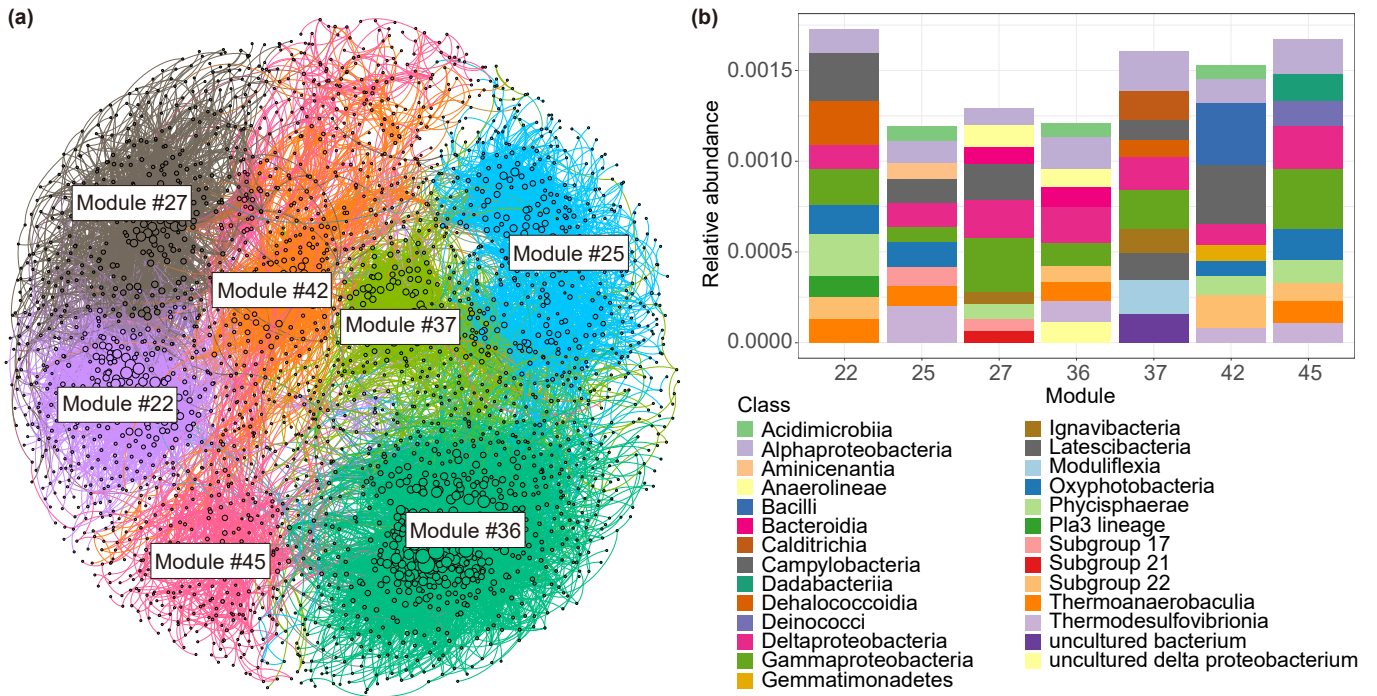
903 Zhang, G., Bai, J., Zhao, Q., Jia, J., Wang, W., & Wang, X. (2020). Bacterial
904 succession in salt marsh soils along a short-term invasion chronosequence of
905 *Spartina alterniflora* in the Yellow River Estuary, China. *Microbial Ecology*, 79,
906 644–661. <https://doi.org/10.1007/s00248-019-01430-7>

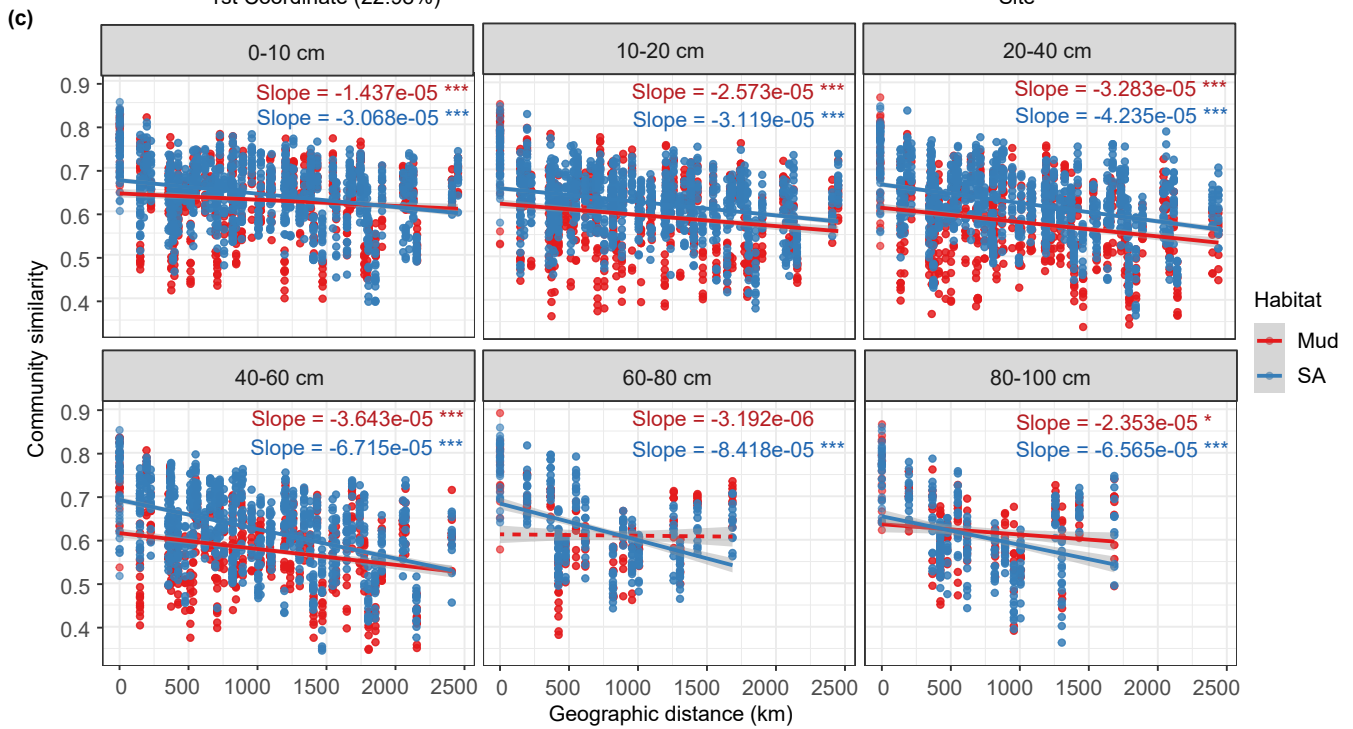
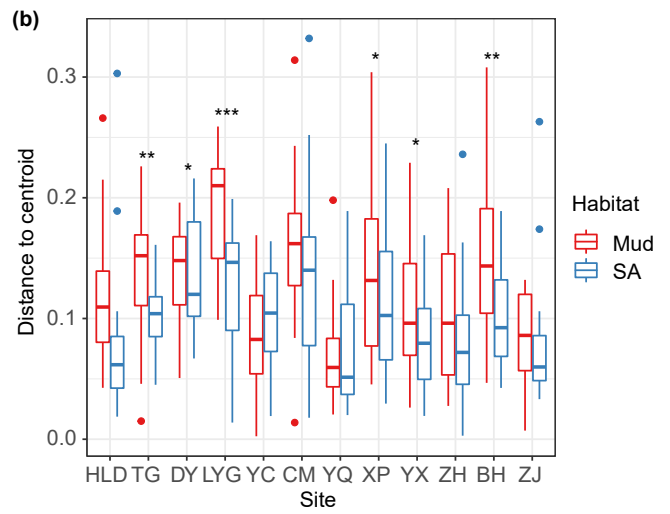
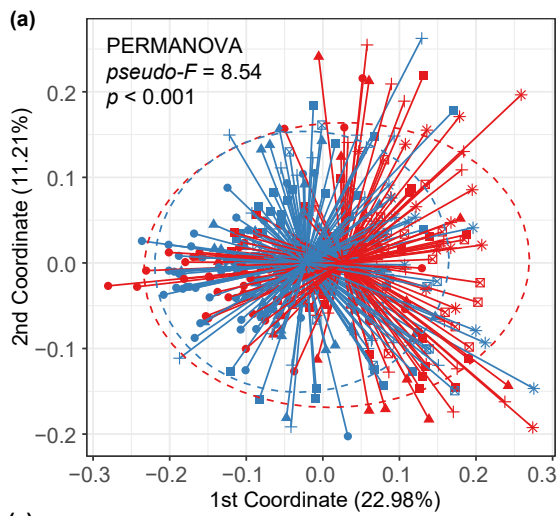
907 Zhang, Y., Pennings, S. C., Li, B., & Wu, J. (2019). Biotic homogenization of
908 wetland nematode communities by exotic *Spartina alterniflora* in China.
909 *Ecology*, 100(4), e02596. <https://doi.org/10.1002/ecy.2596>

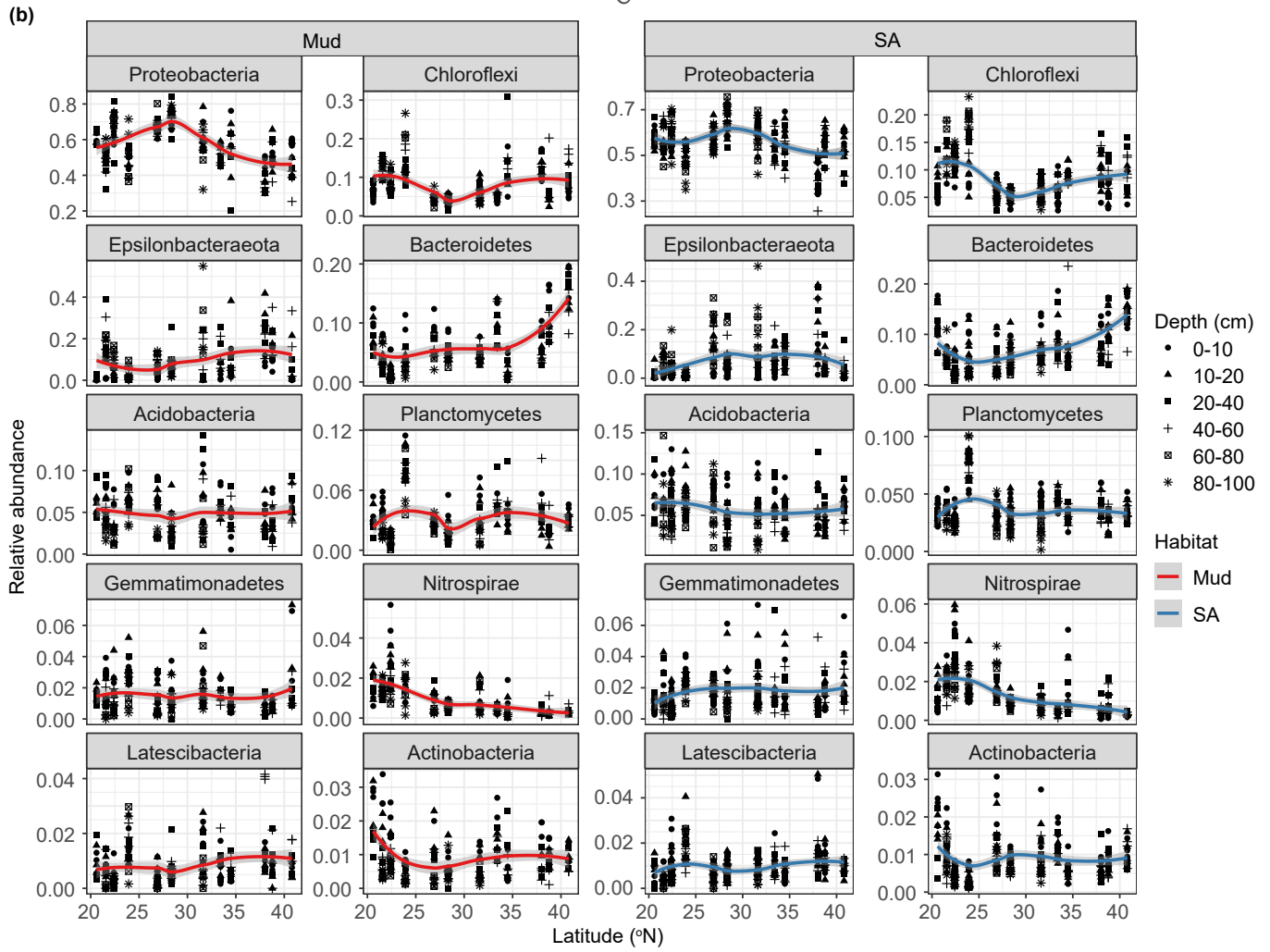
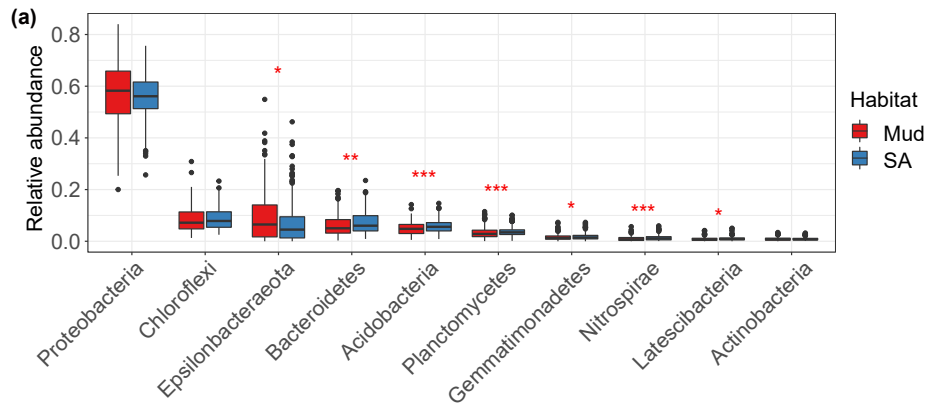
910 Zuo, P., Zhao, S., Liu, C., Wang, C., & Liang, Y. (2012). Distribution of *Spartina* spp.
911 along China's coast. *Ecological Engineering*, 40, 160–166.
912 <https://doi.org/10.1016/j.ecoleng.2011.12.014>

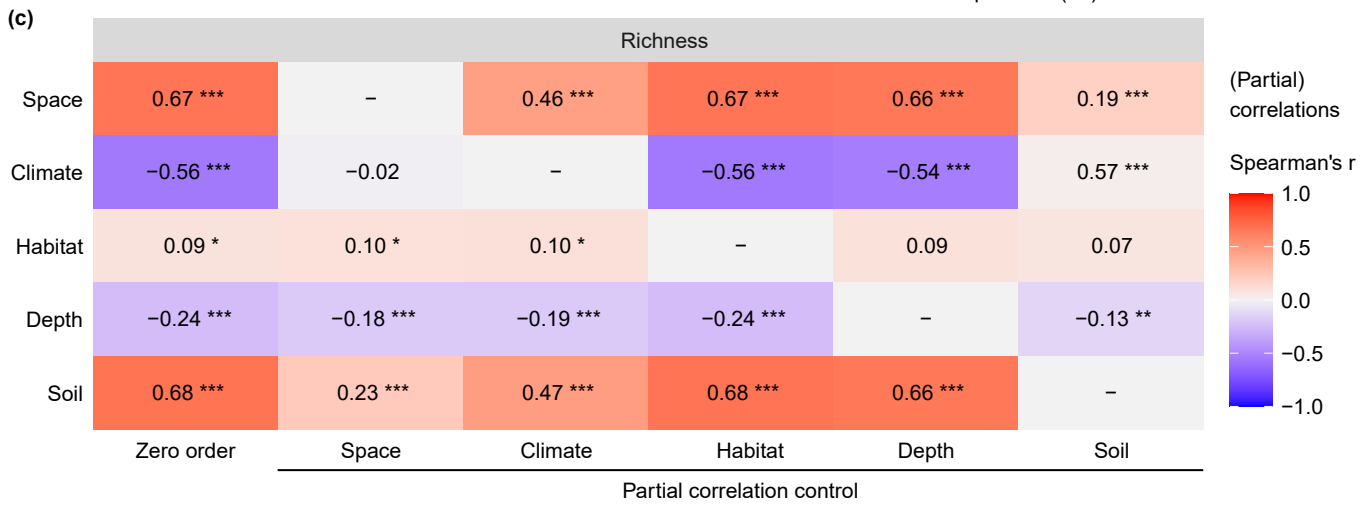
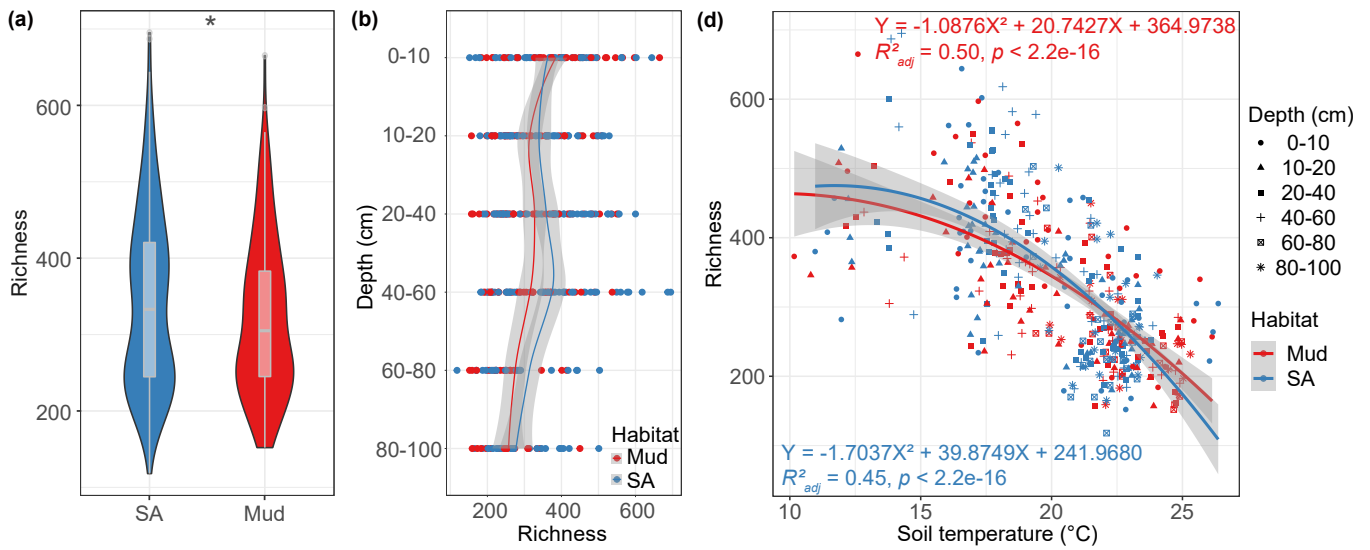
913

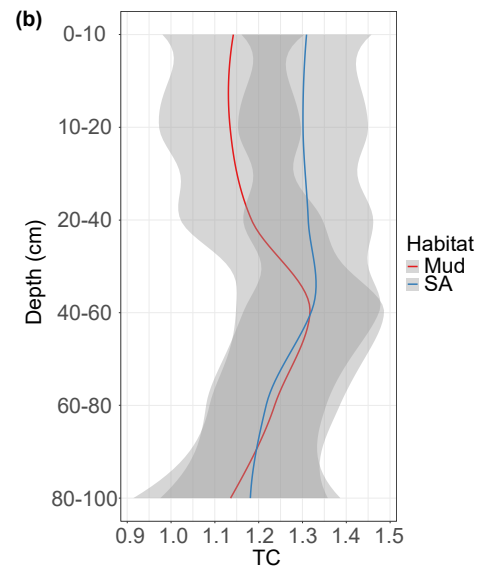
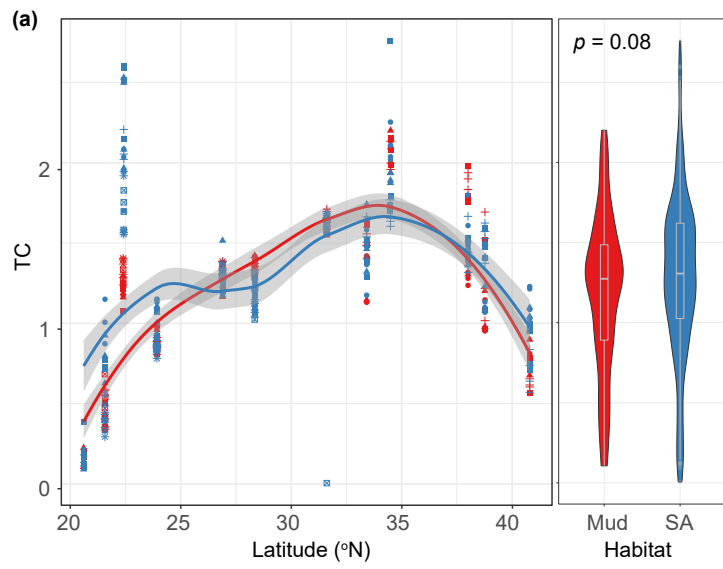


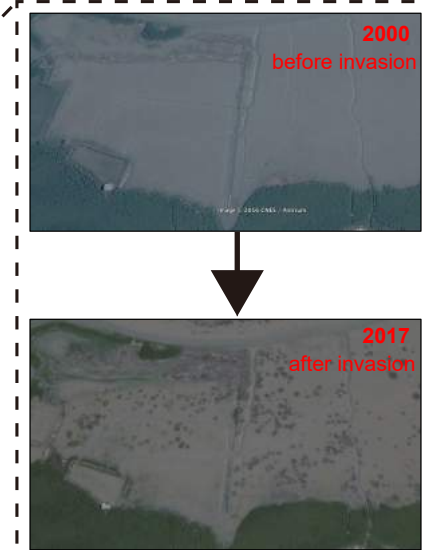
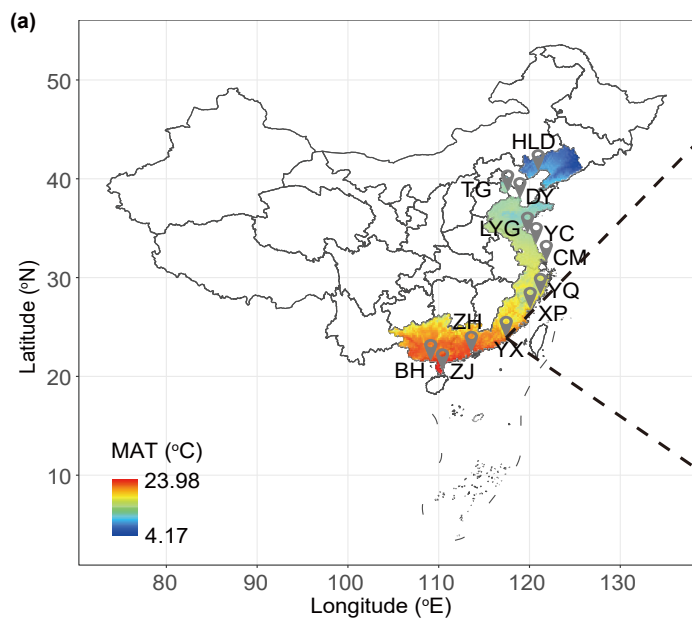




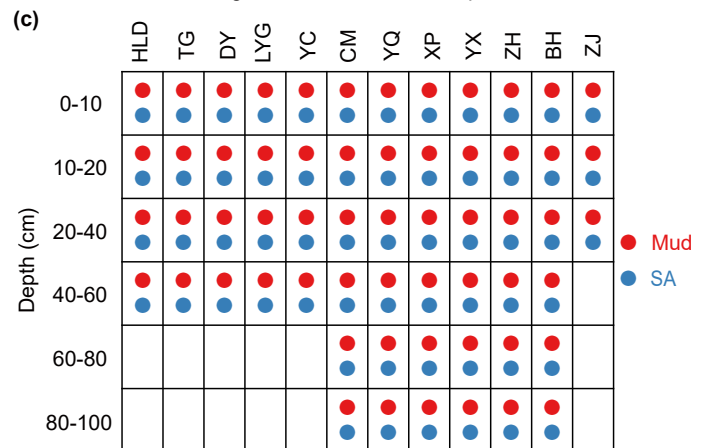
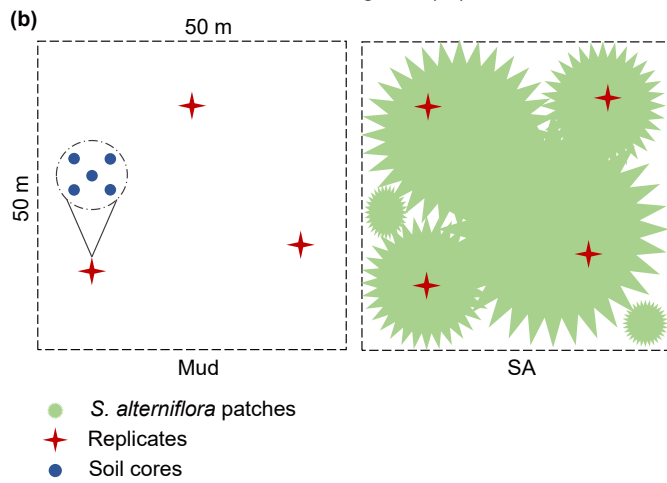








Comparison before and after plant invasion, taking the YX site as an example.



Title page

Types of contribution: Research articles

Continental-scale plant invasions reshuffle the soil microbiome of blue carbon ecosystems

Authors: Gui-Feng Gao^{1, 2, 3, #}, Huan Li^{3, 4, #}, Yu Shi⁵, Teng Yang^{1, 2}, Chang-Hao Gao³, Kunkun Fan^{1, 2}, Yihui Zhang³, Yong-Guan Zhu⁶, Manuel Delgado-Baquerizo^{7, 8, *}, Hai-Lei Zheng^{3, *}, Haiyan Chu^{1, 2, *}

¹ State Key Laboratory of Soil and Sustainable Agriculture, Institute of Soil Science, Chinese Academy of Sciences, 71 East Beijing Road, Nanjing 210008, China

² University of Chinese Academy of Sciences, Beijing 100049, China

³ Key Laboratory of the Ministry of Education for Coastal and Wetland Ecosystems, College of the Environment and Ecology, Xiamen University, Xiamen 361102, China

⁴ College of Food and Bio-engineering, Bengbu University, Bengbu 233030, China

⁵ State Key Laboratory of Crop Stress Adaptation and Improvement, School of Life Sciences, Henan University, Kaifeng 475004, China

⁶ Key Laboratory of Urban Environment and Health, Institute of Urban Environment, Chinese Academy of Sciences, Xiamen 361021, China

⁷ Laboratorio de Biodiversidad y Funcionamiento Ecosistemico. Instituto de Recursos Naturales y Agrobiología de Sevilla (IRNAS), CSIC, Av. Reina Mercedes 10, E-41012, Sevilla, Spain.

⁸ Unidad Asociada CSIC-UPO (BioFun). Universidad Pablo de Olavide, 41013 Sevilla, Spain.

These authors contributed equally to this work.

* Corresponding authors:

Haiyan Chu, hychu@issas.ac.cn

Hai-Lei Zheng, zhenghl@xmu.edu.cn

Manuel Delgado-Baquerizo, m.delgadobaquerizo@gmail.com

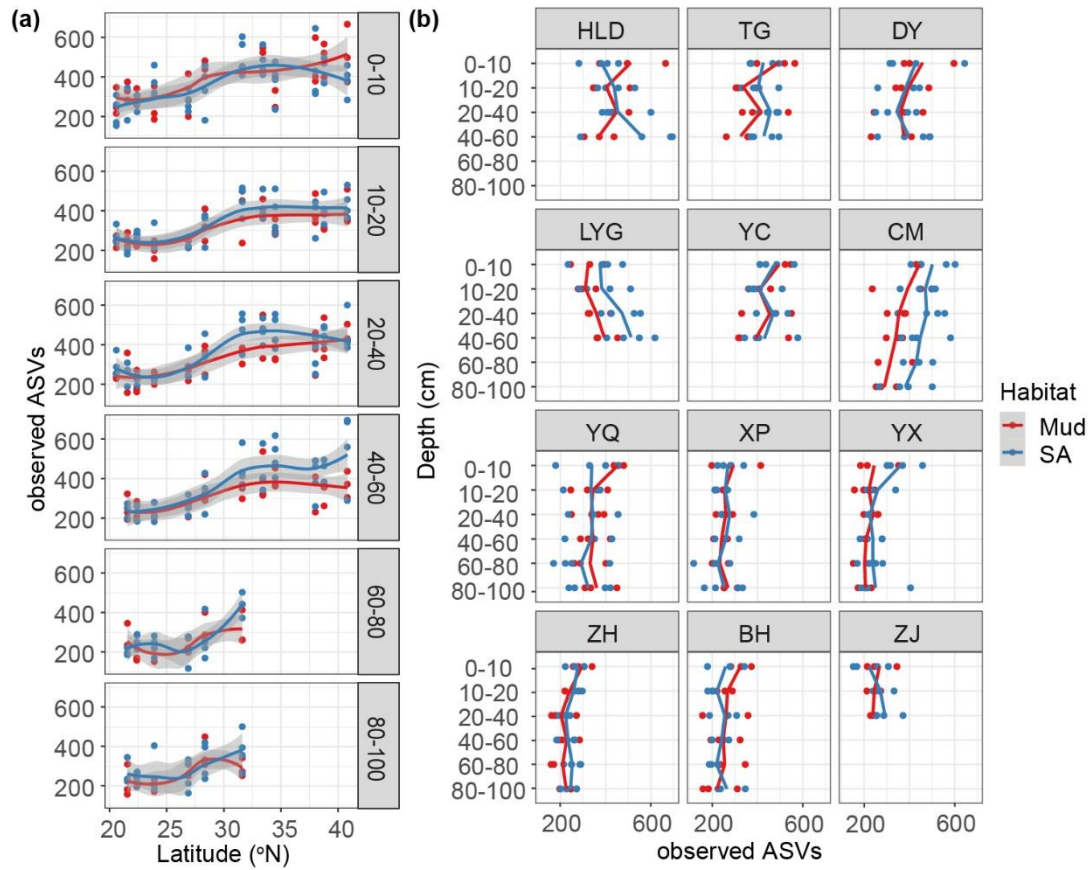


Fig. S1 Changes of soil bacterial alpha diversity. Variations of observed ASVs in various depths with latitude (a). Variations of observed ASVs with soil depth in each site (b). Mud: bare mudflat; SA: *Spartina alterniflora*; HLD: Huludao; TG: Tanggu; DY: Dongying; LYG: Lianyungang; YC: Yancheng; CM: Chongming; YQ: Yueqing; XP: Xiapu; YX: Yunxiao; ZH: Zhuhai; BH: Beihai; ZJ: Zhanjiang.

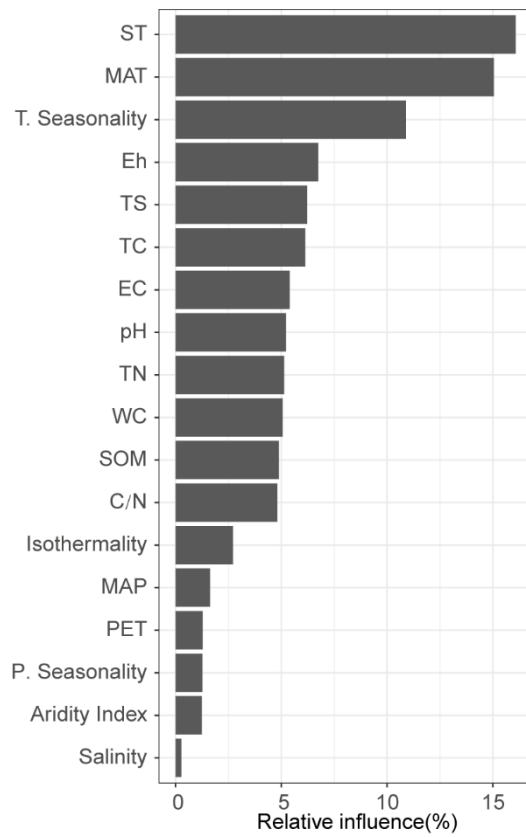


Fig. S2| Random forest analysis was used to identify the key environmental factors in affecting observed ASVs. The relative importance of the environmental factors was ranked in a descending order. ASVs: amplicon sequence variants; Eh: redox potential; ST: soil temperature; EC: electrical conductivity; TN: total nitrogen; TC: total carbon; TS: total sulfur; SOM: soil organic matter; WC: water content; MAP: mean annual precipitation; MAT: mean annual temperature; PET: potential evapotranspiration.

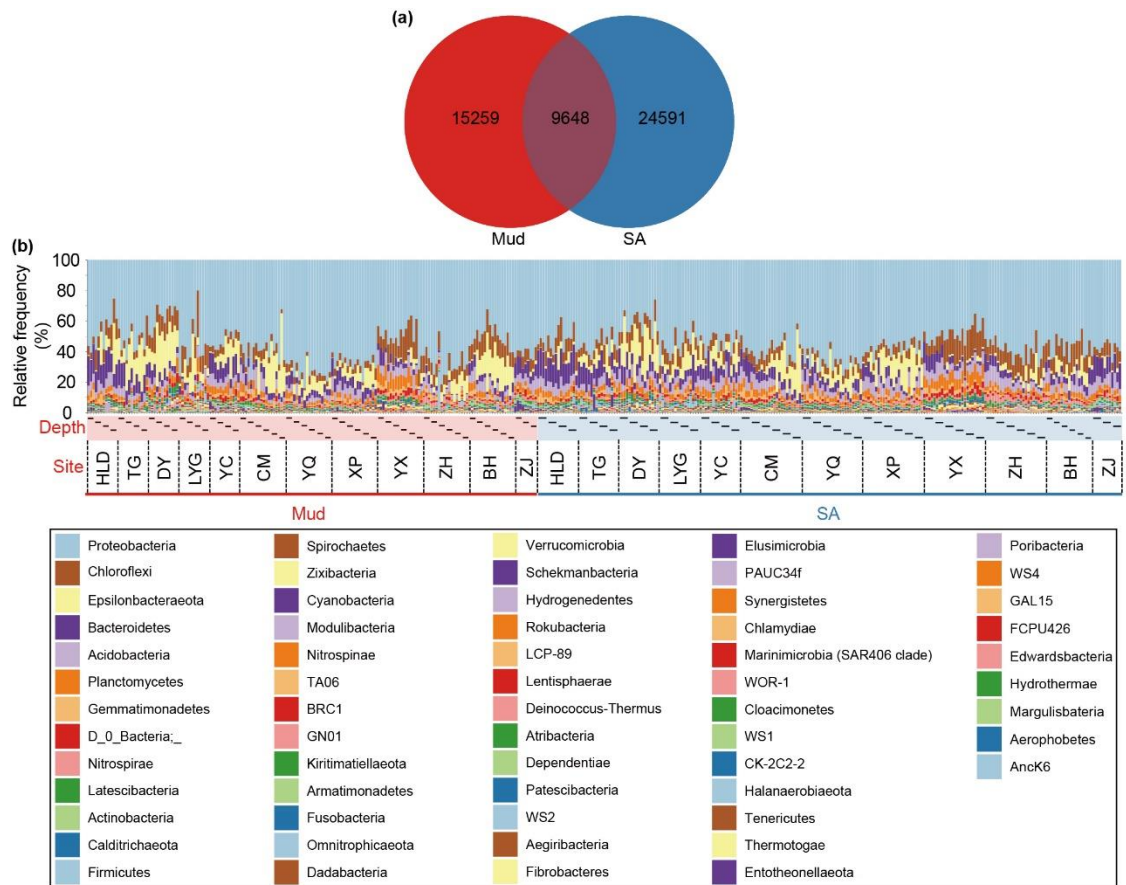


Fig. S3 | The number of unique and shared ASVs of Mud and SA habitats (a). The relative abundance of identified bacterial phyla (b). Different colors of the columns represent different bacterial phyla. For abbreviations, see the legends of Fig. S1.

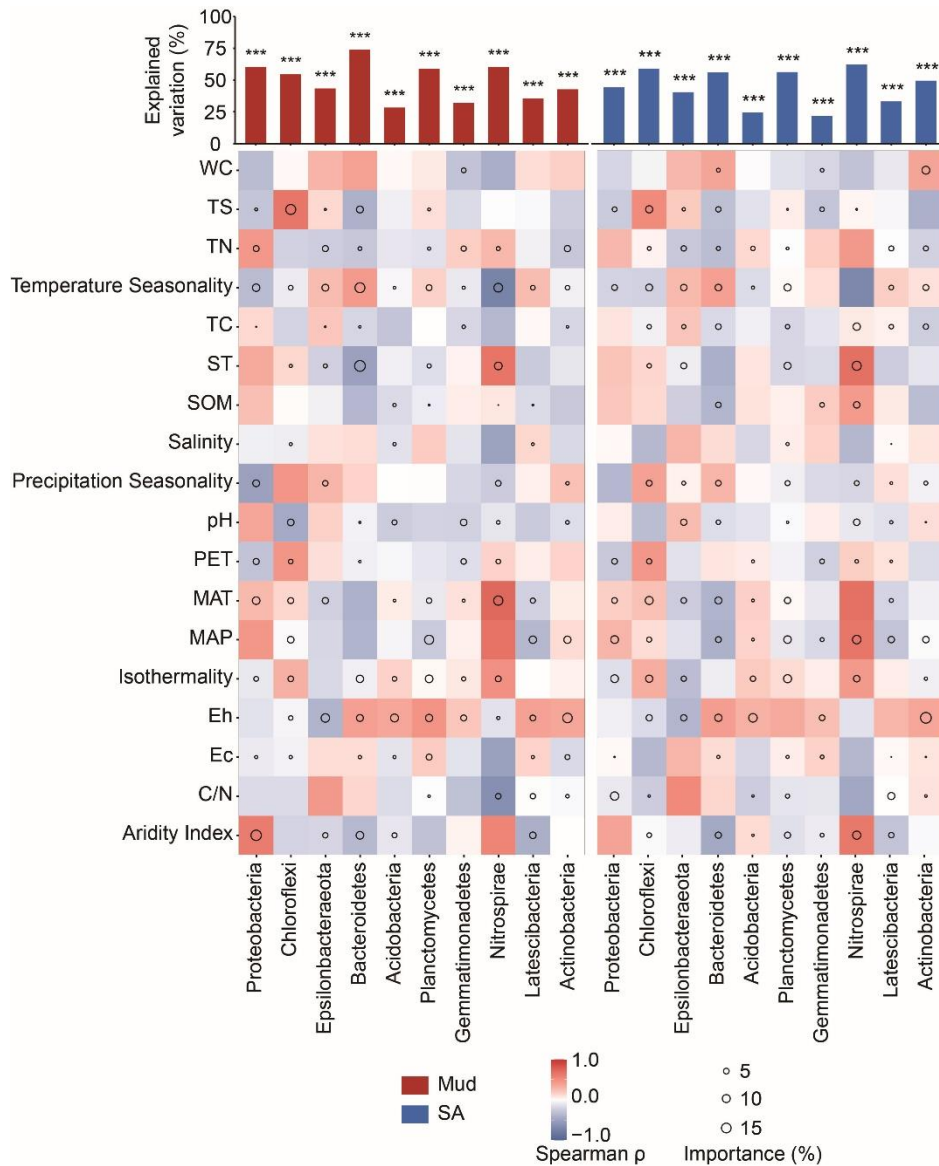


Fig. S4 Contributions of soil properties to the differences in relative abundances of microbial phyla based on correlation and best multiple regression model. The heat map represents the Spearman correlation coefficients between soil properties and phyla. The bars represent the total contribution of soil properties in explaining microbial variation, and the circle size indicates the importance of soil properties, which is obtained by multiple linear regression and variance decomposition analysis. For abbreviations, see the legends of Fig. S1 and Fig. S2. * $p < 0.05$; ** $p < 0.01$; *** $p < 0.001$.

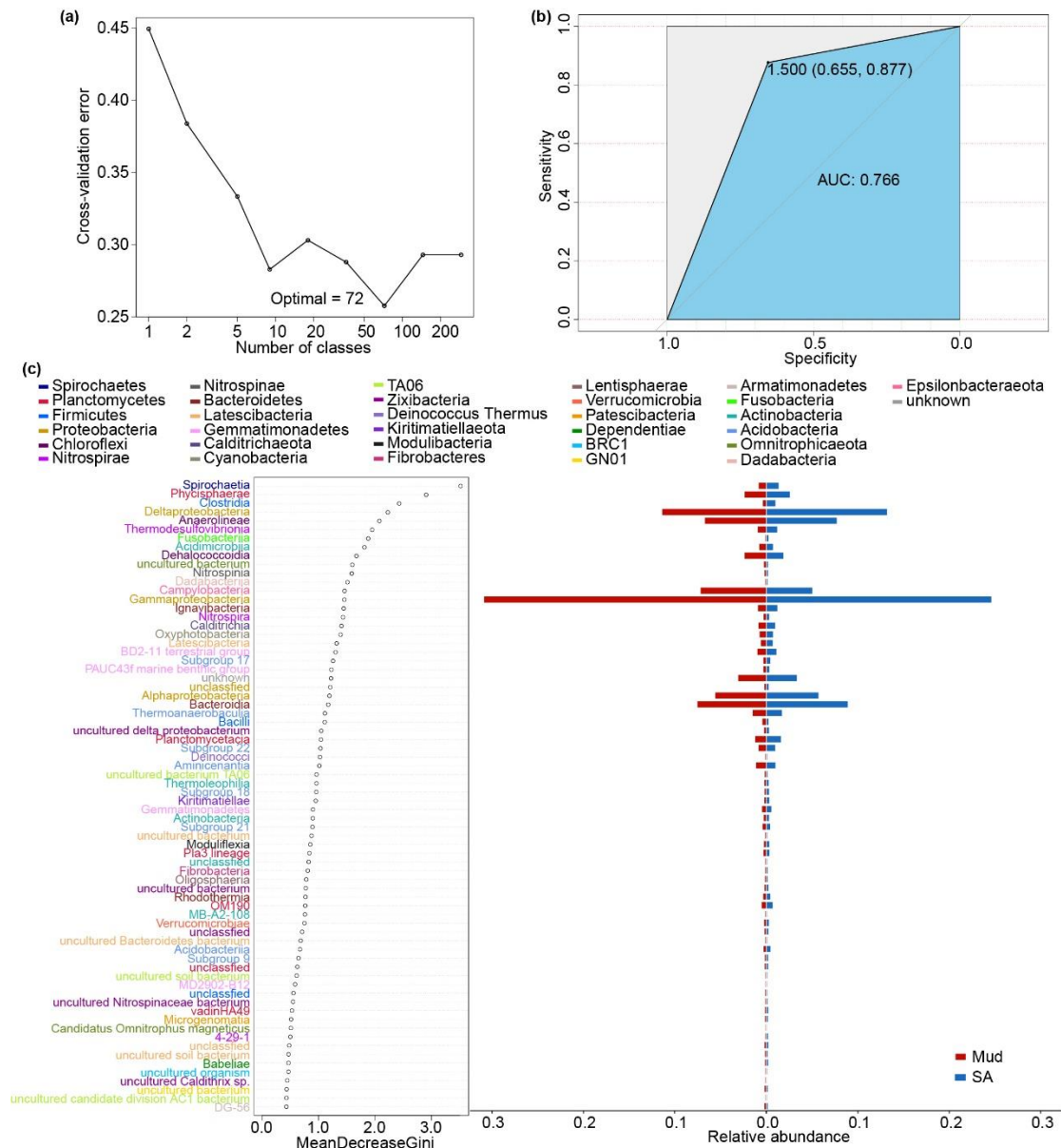


Fig. S5 Random Forest analysis demonstrating biomarkers in Mud and SA soils. The cross-validation error as a function of the number of input classes used to classify against group (a). AUC score for evaluation of random forest classification models (b). Biomarkers ranking in a descending order of their importance to the accuracy of the model (c). The colors of the classes represent the phyla to which they belong to. For abbreviations, see the legends of Fig. S1.

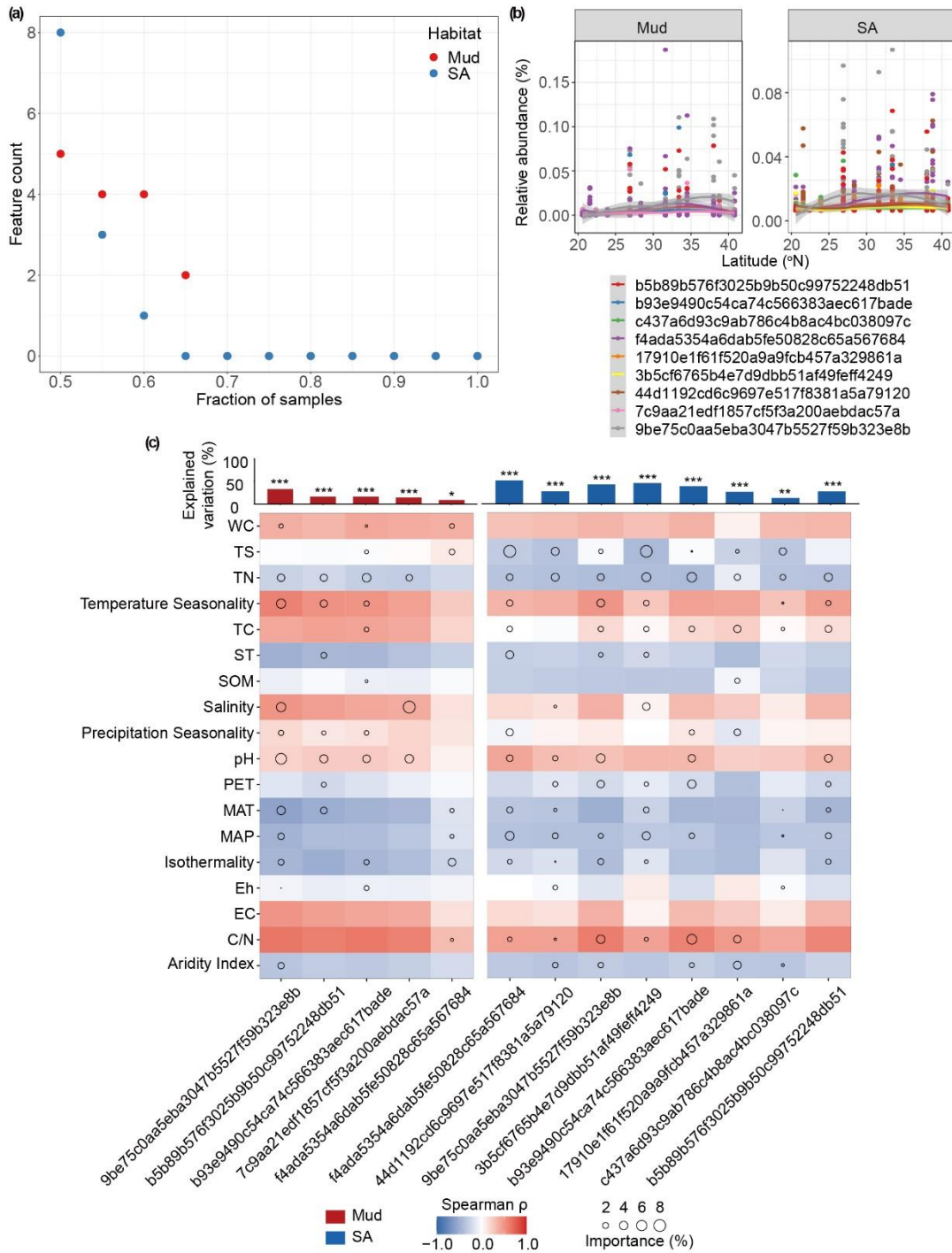


Fig. S6 Identification of core species. Relationship between changes in the number of core species and their proportional occurrence in the samples (a). Variation in relative abundance of core species with latitude (b). Contributions of soil properties to the differences in relative abundances of core species based on correlation and best multiple regression model. The heat map represents the Spearman correlation coefficients between soil properties and core species. The bars represent the total contribution of soil properties in explaining microbial variation, and the circle size indicates the importance of soil properties, which is obtained by multiple linear regression and variance decomposition analysis (c). For abbreviations, see the legends of Fig. S1 and Fig. S2.

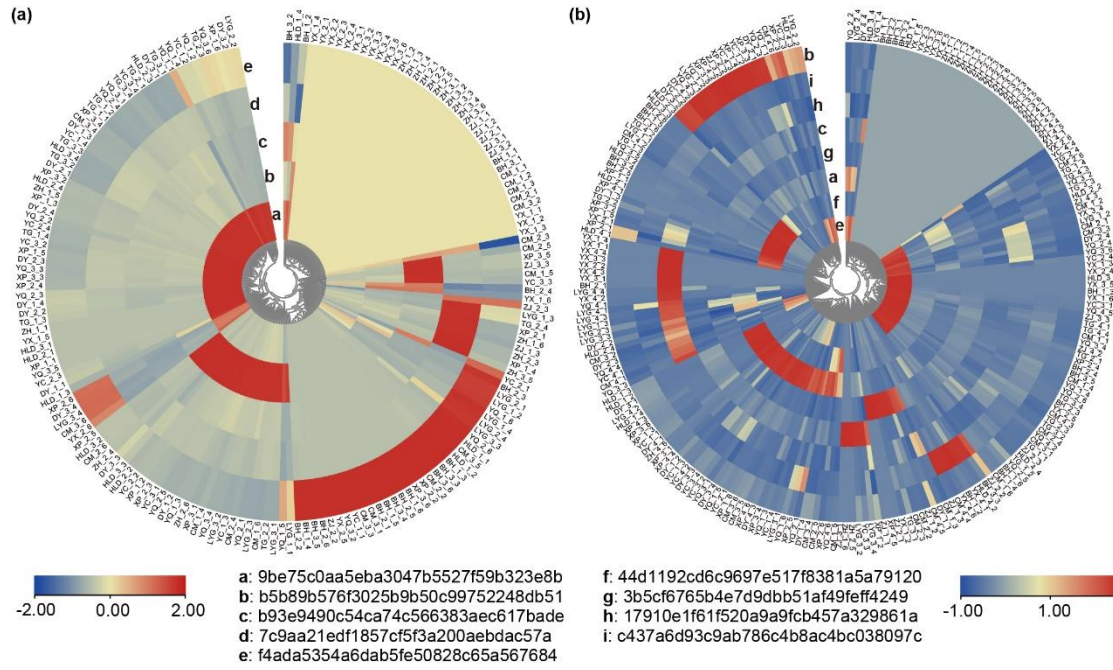


Fig. S7 Heat map showing the relative abundance of core species in all samples for Mud (a) and SA (b) soils. The lower-case letters in the diagram represent their corresponding ASVs. For abbreviations, see the legends of Fig. S1.

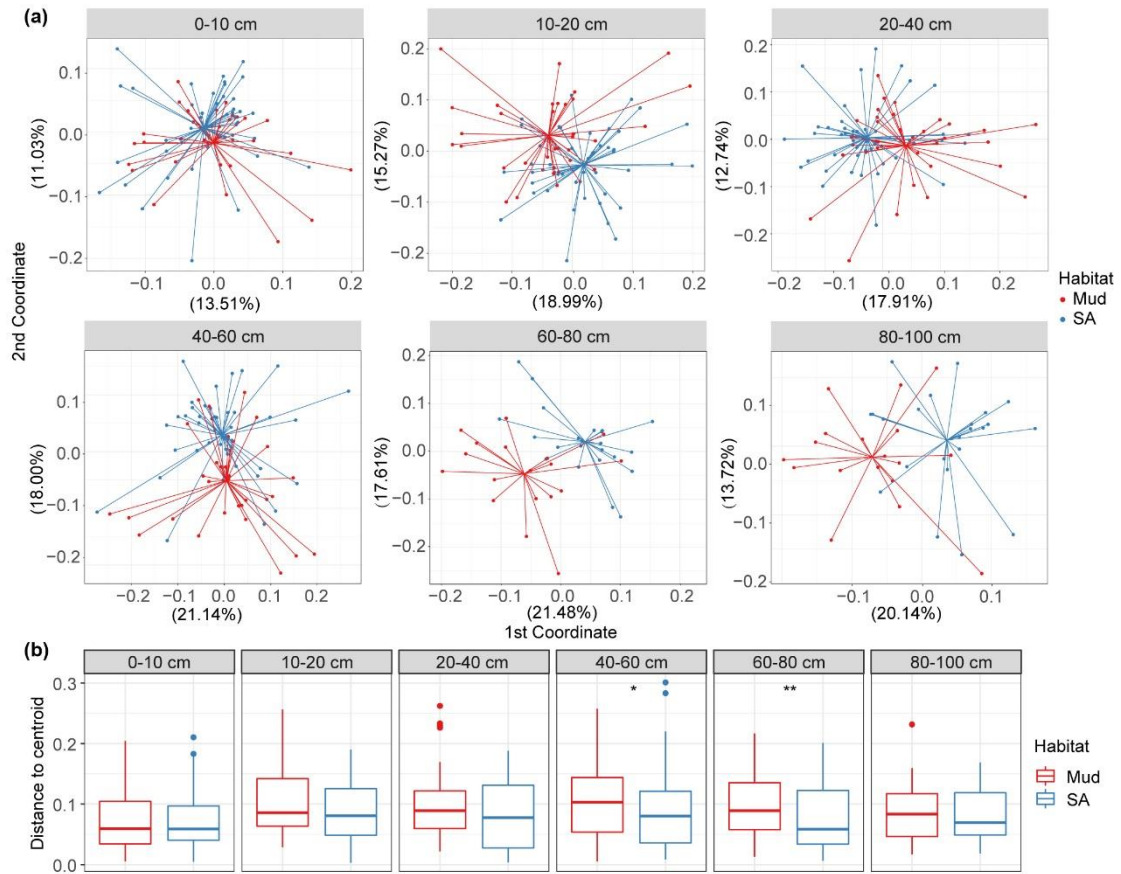


Fig. S8 Results of the covariate adjusted principal coordinates analysis (aPCoA) based on the Weighted UniFrac distance revealing the pairwise dissimilarities between Mud and SA habitats for each soil depth (a). Distance of soil bacterial community to centroid point for each soil depth (b). For abbreviations, see the legends of Fig. S1. * $p < 0.05$; ** $p < 0.01$; *** $p < 0.001$.

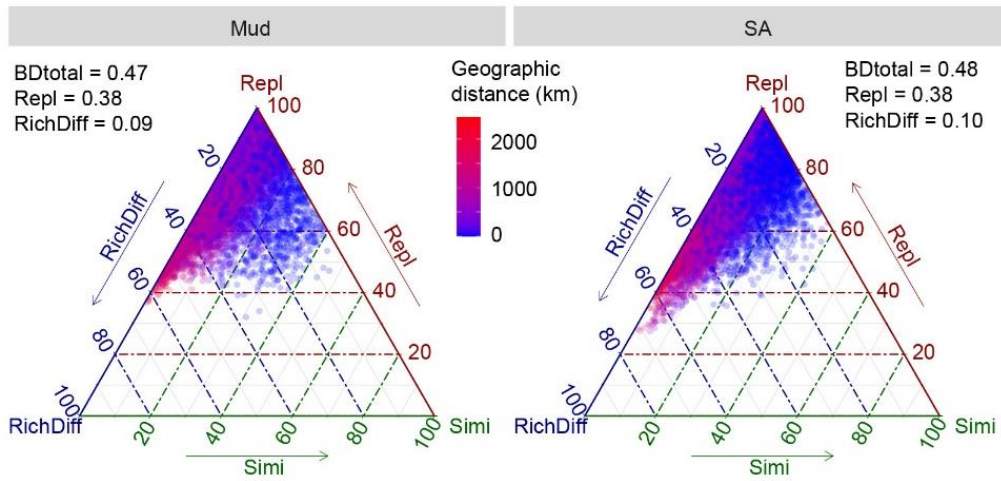


Fig. S9 | Variation in the relative contribution of beta diversity components with geographic distance. For abbreviations, see the legends of Fig. S1.

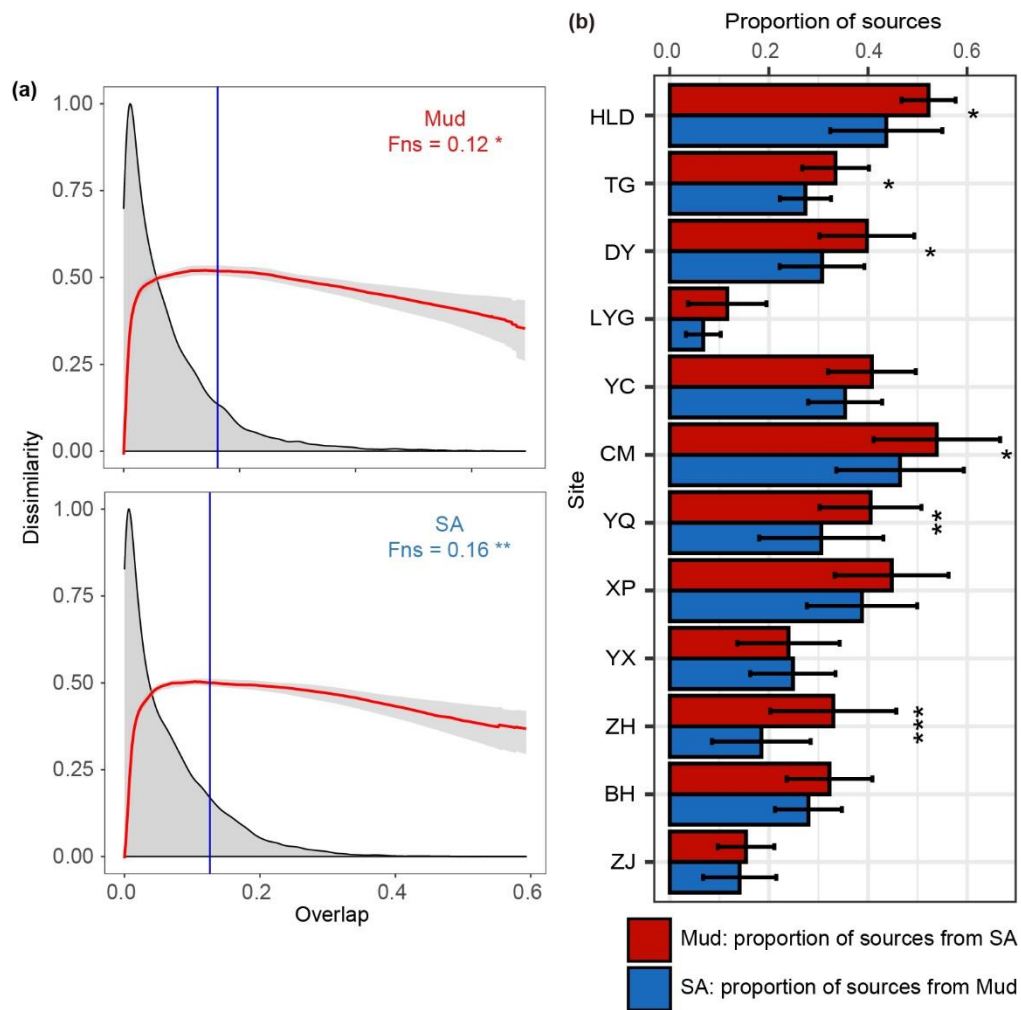


Fig. S10 Dissimilarity Overlap curve was used to examine whether the ecological dynamics of the bacterial communities are universal across all communities or unique to individual communities (a). Fast expectation-maximization microbial source tracking (FEAST) analysis reveals the proportion of sources in Mud or SA habitats, respectively (b). For abbreviations, see the legends of Fig. S1. * $p < 0.05$; ** $p < 0.01$; *** $p < 0.001$.

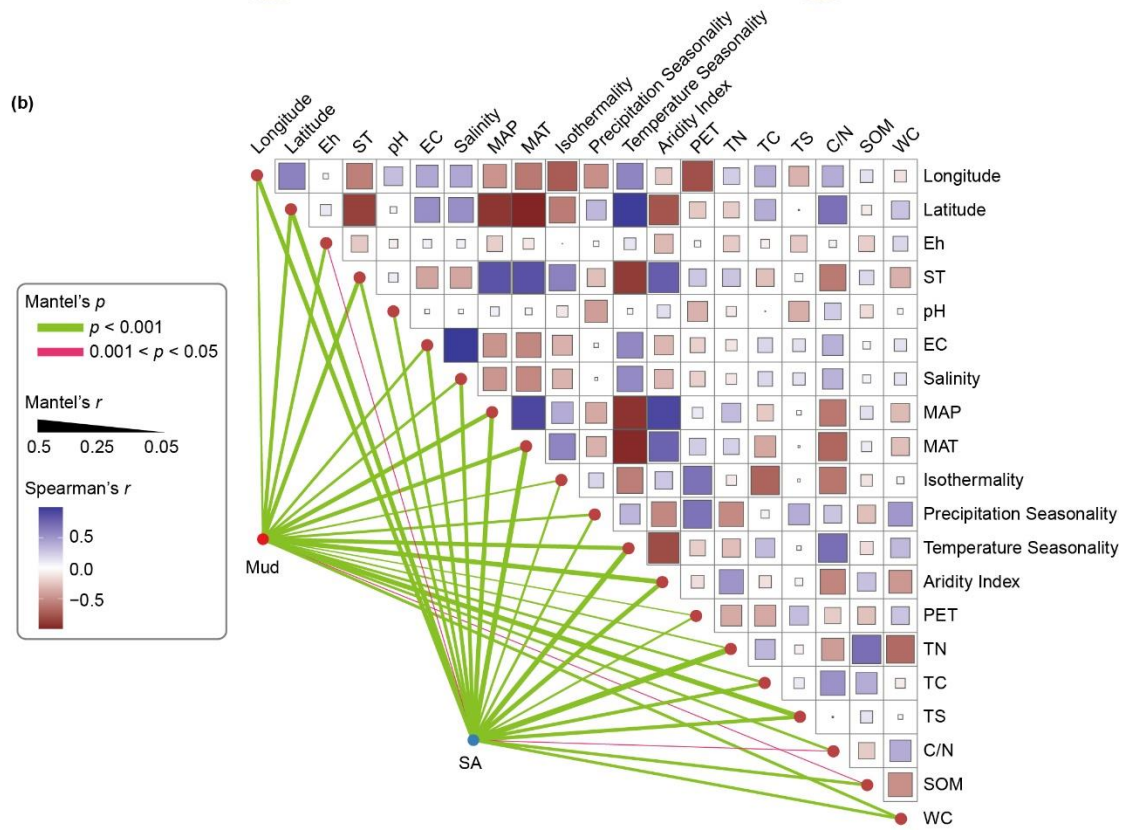
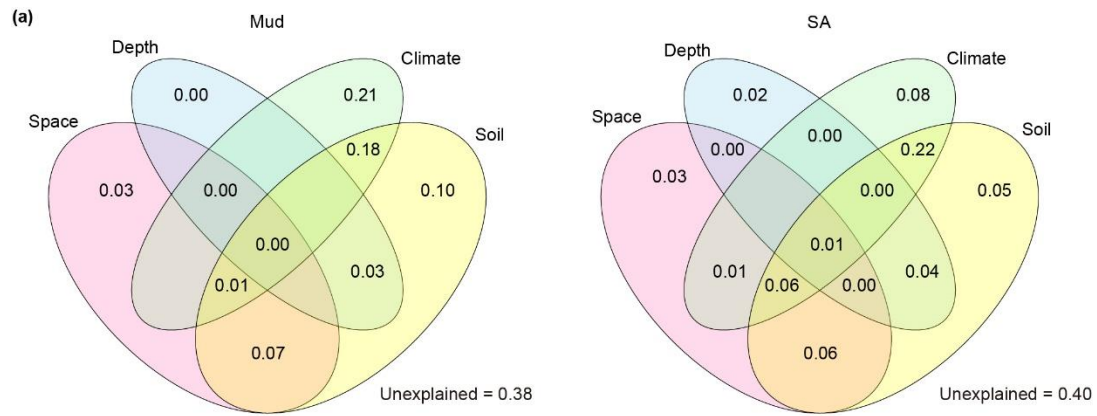


Fig. S11 | The results of variation partitioning analysis (VPA) showed the dependent and independent effects of space, depth, climate and soil factors in influencing bacterial communities (a). The Spearman correlations between environmental factors, and the Mantel correlations between bacterial communities and soil properties, for Mud and SA habitats respectively. The thickness and the color of the line represents the magnitude of the Mantel's r and p value (b). For abbreviations, see the legends of Fig. S1 and Fig. S2.

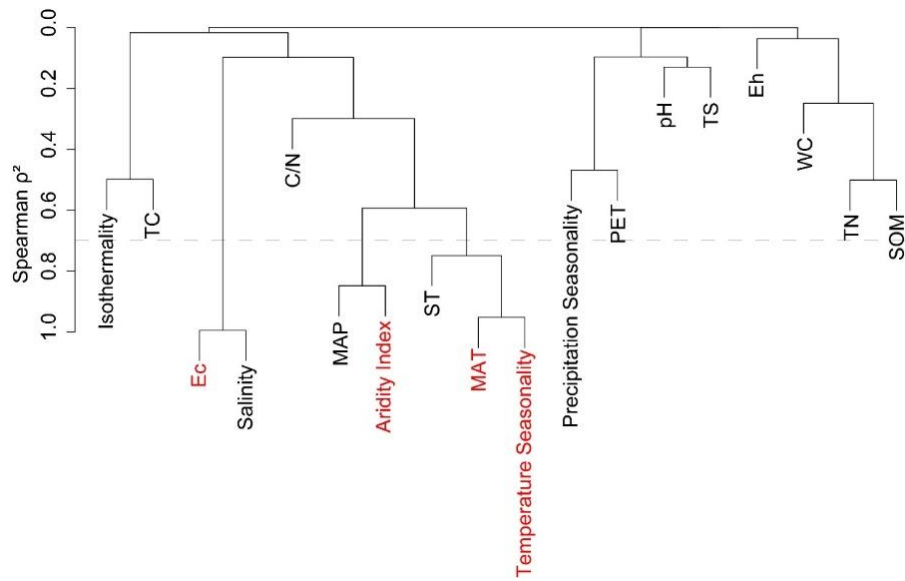


Fig. S12 | To avoid the effect of multicollinearity, the redundancy of environmental variables was evaluated. The dashed line is Spearman ρ^2 equal to 0.7, and the environment variables marked in red font are those deleted in the subsequent analysis. For abbreviations, see the legends of Fig. S2.

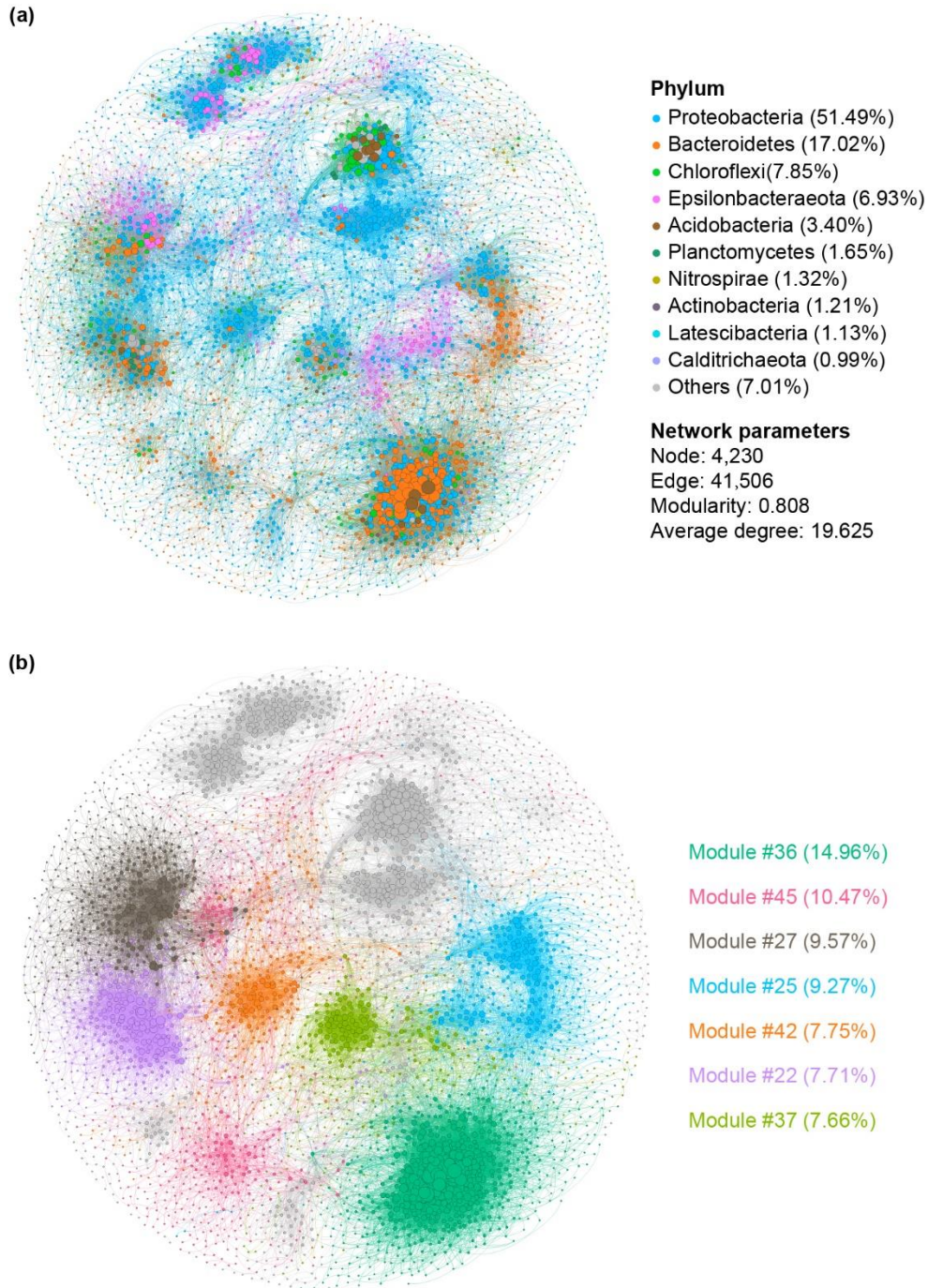


Fig. S13 Co-occurrence network of soil bacterial communities. The colors of the nodes represent the different dominant bacterial phyla (a). The percentage in parentheses represents the percentage of bacteria of that phylum within the network. The color of the nodes represents the different ecological modules (b). Modules with more than 300 nodes are marked with different colors. The percentage in parentheses represents the percentage of that module within the network.

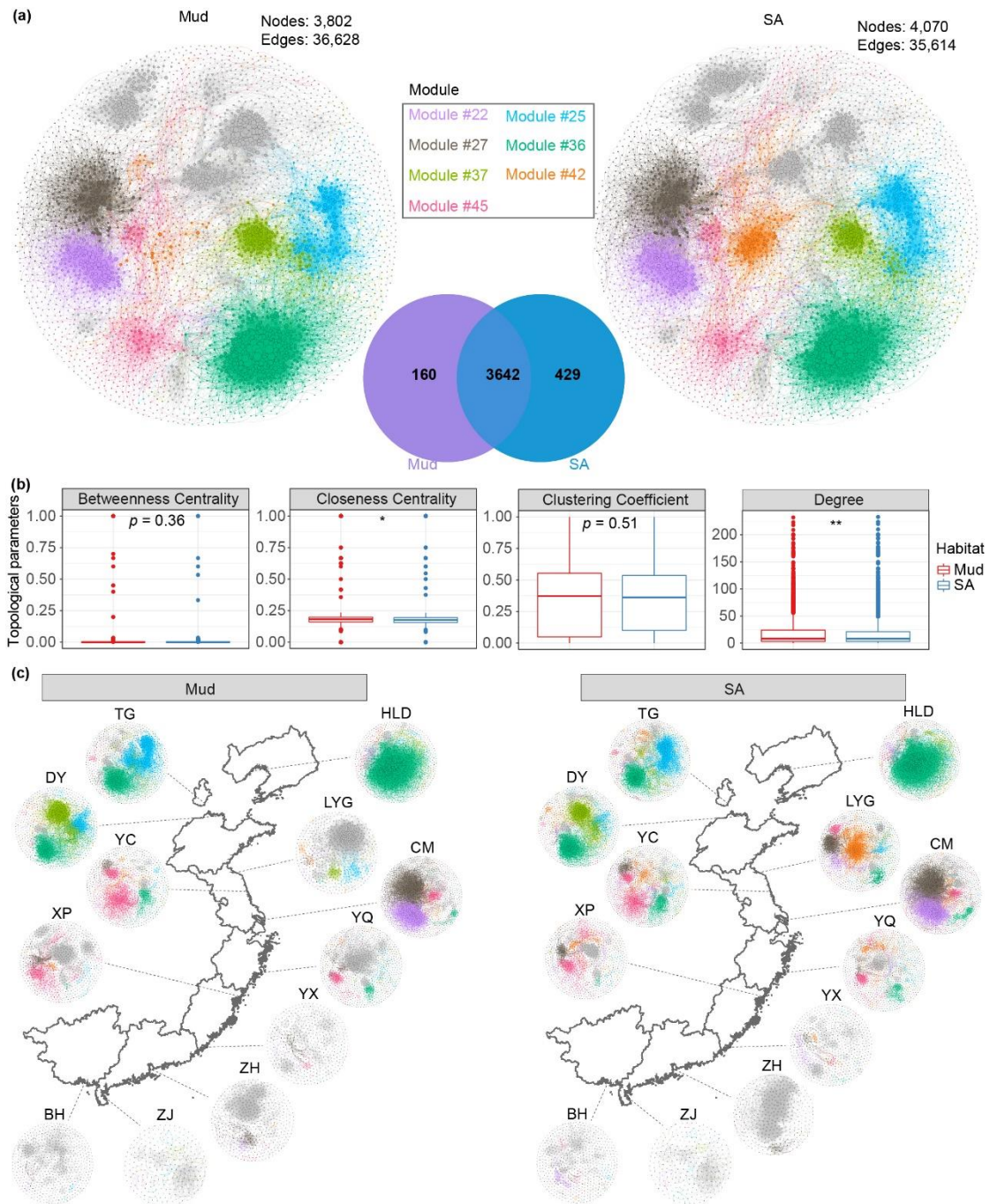


Fig. S14 | Bacterial co-occurrence network for Mud and SA soils respectively. Venn diagram showing the number of unique and shared ASVs for Mud and SA networks (a). The color of the nodes represents the different ecological modules. The differences of topological parameters between Mud and SA networks (b). The latitudinal distribution of co-occurrence network for Mud and SA soils respectively (c). $p < 0.05$ *; $p < 0.01$ **. For abbreviations, see the legends of Fig. S1.

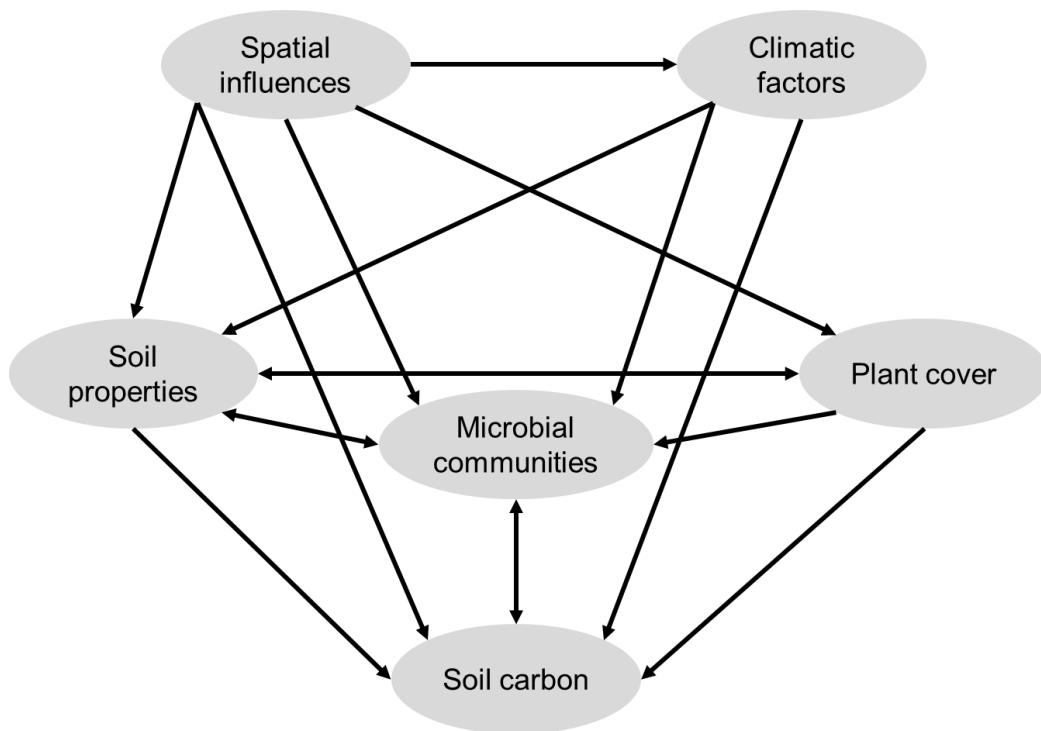


Fig. S15 The initial model of structure equation modeling analysis. The arrows indicate the predicted causal relationships.

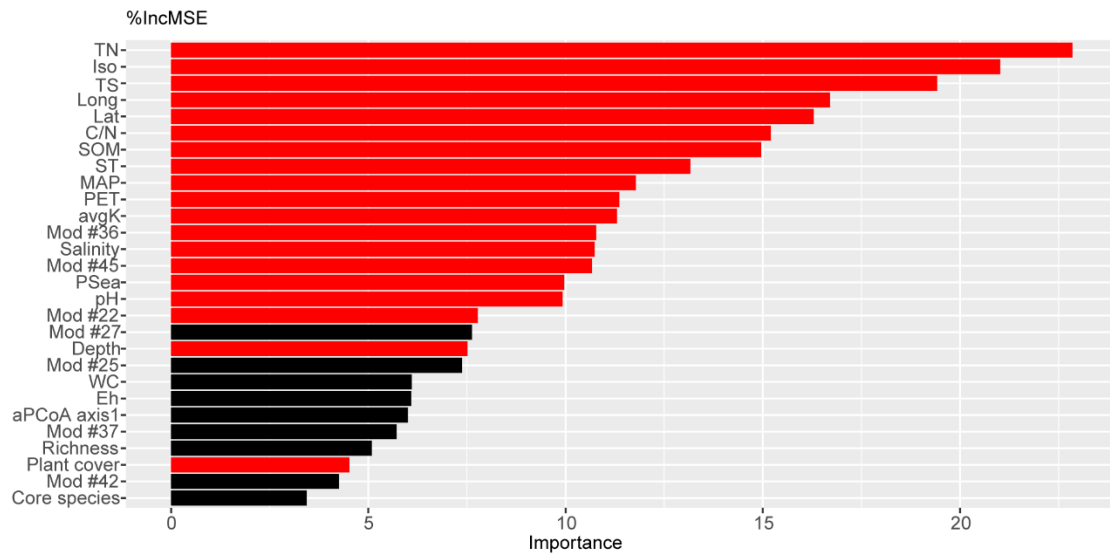


Fig. S16 Random Forest analyses were conducted to identify the most important predictors in influencing soil TC. The graphic shows importance scores scaled by ranked importance. For abbreviations, see the legends of Fig. S2.